

New Mode (Molecular-Sensing) of Heinz Body Formation Mechanisms Inherent in Human Erythrocytes: Basis for Understanding of Clinical Aspects of Drug-Induced Hemolytic Anemia and the Like

Yoshiaki Sugawara*, Yuki Shigemasa, Yuko Hayashi, Yoko Abe, Ikumi Ohgushi and Eriko Ueno

Department of Health Science, Prefectural University of Hiroshima, Hiroshima 734-8558, Japan

Abstract

The human hemoglobin (Hb) molecule ($\alpha_2\beta_2$) has two types of α - β interface (*i.e.*, α_1 - β_1 [and α_2 - β_2] and α_1 - β_2 [and α_2 - β_1]). The latter α_1 - β_2 (and α_2 - β_1) interface is associated with cooperative O_2 binding, and exhibits principal roles if the molecule goes from its deoxygenated to oxygenated quaternary structure. The role of the former α_1 - β_1 (and α_2 - β_2) interface has been unclear for a long time. In this regard, important and intriguing observations have been accumulating, so that a new gaze can be focused on the α_1 - β_1 (and α_2 - β_2) interface. Our most recent findings suggest that the α_1 - β_1 (and α_2 - β_2) interface may exert delicate control of the intrinsic tilting capability of the distal (E7) His residues (*i.e.*, $\alpha 58$ His (E7) in the α chain and $\beta 63$ His (E7) in the β chain) depending on internal and external conditions of the erythrocyte to lead to degradation of Hb to hemichrome, and subsequent clustering of Heinz bodies within the erythrocyte. In the spleen, rigid intra-erythrocytic hemichrome inclusions (Heinz bodies) act as "sticking points", so Heinz body-containing red cells become trapped and undergo hemolysis. In this article, we first provide our necessary basic experimental findings that led us to grasp molecular biosensing mechanisms inherent in human erythrocytes for the appreciation of aging and determination of their lifespan, and summarize their roles in physiology. We then discuss how these accomplishments contribute to deeper understanding of clinical aspects of drug-induced hemolytic anemia, defects in the intra-erythrocytic reducing system and unstable Hb disease, in which the mechanisms for acute hemolytic crisis cannot be explained on the basis of conventional views.

Keywords: Red cell aging; Hemichrome formation; Heinz-body clustering; Drug-induced hemolytic anemia; Defects in the intra-erythrocytic reducing system; Unstable hemoglobin disease

Introduction

Human red blood corpuscles survive in the circulation for an average of 120 days. Removal of aged and damaged red cells from the blood circulation is essential for its homeostasis. How do human erythrocytes appreciate aging and determine their lifespan? In a series of studies, we have attempted to examine the relationship between the oxidative behavior of human hemoglobin (Hb) molecules (*i.e.*, oxidation of HbO₂ by the bound O₂ to the ferric met-form), hemichrome emergence and the formation of Heinz bodies within the erythrocytes.

Heinz bodies are intra-erythrocytic inclusions of hemichrome formed from oxidized or denatured hemoglobin (Hb). Heinz bodies are typically formed in aged red cells [1]. However, they are rarely mentioned in the context of normal Hb or normal erythrocytes. Heinz bodies have been characterized in drug-induced hemolytic anemia, defects in the intra-erythrocytic reducing system (e.g., glucose 6-phosphate dehydrogenase [G-6-PD] deficiency) and in unstable Hb disease [2,3]. Nevertheless, Heinz bodies in normal erythrocytes are of interest because they (or their related intra-erythrocytic inclusions) are involved in the recognition mechanisms in the spleen responsible for the removal of non-functional erythrocytes from the circulation. The rigid intra-erythrocytic hemichrome inclusions are known to act as "sticking points", and hence Heinz body-containing red cells become trapped and undergo hemolysis [4].

Hemichrome is rarely found in erythrocytes *in situ*, even though the reaction dynamics of Hb with molecular oxygen (O₂) make them particularly suitable O₂ carriers. Hb can bind O₂ in the ferrous state to carry out its physiological functions. During this reversible binding of O₂, the oxygenated form of Hb (HbO₂) is known to be oxidized by the bound O₂ to the ferric met form (metHb), which cannot be oxygenated,

and is thus physiologically inactive. The resultant met Hb is reduced back to the ferrous state by an intra-erythrocytic nicotinamide adenine dinucleotide (NADH)-dependent reducing system [5-7]. However, it has been suggested that its oxidation (autoxidation) can be followed by transformation of the oxidized molecule (high-spin Fe³⁺) into a species absorbing as a low-spin compound, *i.e.*, hemichrome, the formation of which can result in the accumulation of soluble and insoluble hemichromes as well as precipitation [8-13]. Despite these findings, direct evidence of hemichrome formation in normal erythrocytes is lacking.

Compared with the tetrameric parent Hb, hemichrome formation is enhanced in separated α and β chains [8,13-16]. Following the method of Brunori et al. [14], our ultraviolet/visible (UV/VIS) spectroscopic study [17] showed that human adult Hb (HbAO₂ or simply designated as HbO₂) from healthy donors tended to degrade to produce hemichrome even at close-to-physiological temperatures and pH. However, its occurrence was a function of pH, temperature and the progress of autoxidation of ferrous HbO₂ to the ferric met form through oxidation by bound O₂.

*Corresponding author: Yoshiaki Sugawara, Department of Health Science, Prefectural University of Hiroshima, Hiroshima 734-8558, Japan, Tel: +81-82-251-9783; Fax: +81-82-251-9405; E-mail: sugawara@pu-hiroshima.ac.jp

Received May 02, 2013; Accepted June 12, 2013; Published June 15, 2013

Citation: Sugawara Y, Shigemasa Y, Hayashi Y, Abe Y, Ohgushi I, et al. (2013) New Mode (Molecular-Sensing) of Heinz Body Formation Mechanisms Inherent in Human Erythrocytes: Basis for Understanding of Clinical Aspects of Drug-Induced Hemolytic Anemia and the Like. J Bioanal Biomed 5: 036-056. doi:10.4172/1948-593X.1000078

Copyright: © 2013 Sugawara Y, et al. This is an open-access article distributed under the terms of the Creative Commons Attribution License, which permits unrestricted use, distribution, and reproduction in any medium, provided the original author and source are credited.

Cellular life is reliant upon rapid and efficient responses to internal and external conditions. The basic molecular events associated with these processes are the structural transitions of the proteins involved [18]. Therefore, understanding of the structural basis of protein allostery is of paramount importance to characterize these processes. The human Hb molecule ($\alpha_2\beta_2$; alternatively, a dimer of $\alpha\beta$ protomers), whose α and β chains contain 141 and 146 amino-acid residues, respectively, holds a special position in these structural transitions. This is due to the achievements of Perutz, whose pioneering studies led to the identification of two distinct Hb structures, the tense (T) and relaxed (R) state, which are associated with the deoxygenated and oxygenated form of the protein, respectively [19-21]. Hb has two types of $\alpha\beta$ interface (*i.e.*, $\alpha_1\beta_1$ [and $\alpha_2\beta_2$] and $\alpha_1\beta_2$ [and $\alpha_2\beta_1$]). The latter $\alpha_1-\beta_2$ (and $\alpha_2-\beta_1$) interface is known to be associated with cooperative dioxygen (O_2) binding, and exhibits important roles if the molecule goes from its deoxygenated to the oxygenated quaternary structure. However, the role of the former $\alpha_1-\beta_1$ (and $\alpha_2-\beta_2$) interface has been unclear for a long time.

A representative set of successive O_2 -binding constants regarding human Hb is given in terms of mmHg^{-1} as follows: $K_1 = 0.0188$, $K_2 = 0.0566$, $K_3 = 0.407$, $K_4 = 4.28$ in 0.1 M buffer (pH 7.4) containing 0.1 M KCl at 25°C [22]. In this reaction, by comparing their X-ray crystal structures, major differences have been defined between deoxygenated and oxygenated forms. These include: movement of the iron atom into the heme plane with a simultaneous change in the orientation of the proximal (F8) His; rotation of the $\alpha_1\beta_1$ dimer relative to the other $\alpha_2\beta_2$ dimer about an axis P by 12–15°; and a translation of one dimer relative to the other along the P axis by $\sim 1 \text{ \AA}$ (10^{-1} nm). These changes are accompanied by sequential breaking of “salt bridges” by C-terminal residues [23-27]. When HbO_2 goes from the deoxygenated to the oxygenated quaternary structure, the $\alpha_1-\beta_2$ (and $\alpha_2-\beta_1$) interface undergoes the principal changes associated with cooperative oxygen binding, so it is named the “sliding contact” that involves 19 residues, including mainly helices C and H and the FG corner [25,28].

Conversely, negligible changes are found with respect to the crystal structure examined for the $\alpha_1-\beta_1$ (and $\alpha_2-\beta_2$) interface that associates 35 residues including B, G, and H helices as well as the GH corner. Understanding of subunit interactions between the four Hb chains (and how these explain cooperative O_2 binding) has been the primary focus in Hb research. This has been coupled with a tendency for structural analyses to focus on the changes at the proximal side of the heme and at the $\alpha_1-\beta_2$ (and $\alpha_2-\beta_1$) interface, as mentioned above. This is despite the fact that the configuration of the residues lining the distal side of the heme pocket (where molecular O_2 binds) are also altered by oxygenation, and are thought to have a role in controlling access of the ligand to the heme pocket [29]. Hence, the possibility of subunit interactions originating from or being transmitted *via* distal side effects has, for the most part, been neglected.

In this regard, important and intriguing observations have been accumulating while paying attention to the $\alpha_1-\beta_1$ (and $\alpha_2-\beta_2$) interface as well as distal-side perturbations. Hence, a new gaze could be focused on the $\alpha_1-\beta_2$ (and $\alpha_2-\beta_1$) interface and the distal-side perturbations of the heme pocket. With respect to the $\alpha_1-\beta_1$ (and $\alpha_2-\beta_2$) interface, a new role has been attributed to stabilizing the HbO_2 tetramer against acidic autoxidation. That is, the $\alpha_1-\beta_1$ (and $\alpha_2-\beta_2$) interface produces a conformational constraint in the β chain whereby the distal (E7) histidine (His) residue is tilted slightly away from the bound O_2 so as to prevent proton-catalyzed displacement of O_2^- by a solvent water

molecule [30,31]. The β chains thus acquire pH-dependent delayed autoxidation in the HbO_2 tetramer. The next role was suggested by our studies searching for similar phenomena in normal human erythrocytes under mild heating [17,32,33]. It seemed that tilting of the distal (E7) His in turn triggers degradation of the Hb molecule to hemichrome, and subsequent clustering of Heinzbodies within the erythrocyte. In the spleen, Heinz body-containing red cells become trapped while traversing small apertures in the basement membranes separating the cords from the sinusoids (where the spaces are sufficiently small to require extreme deformation of red cells) and undergo hemolysis [4]. Thus, it was suggested that the Hb molecule controls removal of erythrocytes from the blood circulation by triggering degradation of the Hb molecule to hemichrome, and subsequent clustering of Heinz bodies within the erythrocytes depending on the internal and extraneous conditions of the erythrocyte (including pH and temperature). Hence, in our recent publication [34], we reviewed and summarized current interpretations of the oxidative behavior of human Hb and the related results. We emphasized the correlation between hemichrome emergence and the formation of Heinz bodies within the erythrocytes. In relevance to a clinical aspect, we also suggested that a quite large number of unstable Hbs are resulted from substitutions affecting on the β chain, especially in the $\alpha_1-\beta_1$ (and $\alpha_2-\beta_2$) interface including B, G, and H helices: Tacoma [$\beta 30(\text{B}12)\text{Arg} \rightarrow \text{Ser}$], Abraham Lincoln [$\beta 32(\text{B}14)\text{Leu} \rightarrow \text{Pro}$], Peterborough [$\beta 111(\text{G}13)\text{Val} \rightarrow \text{Phe}$], Madrid [$\beta 115(\text{G}17)\text{Ala} \rightarrow \text{Pro}$], J. Guantanamo [$\beta 128(\text{H}6)\text{Ala} \rightarrow \text{Asp}$], Leslie [$\beta 131(\text{H}9)\text{Gln} \rightarrow \text{deleted}$] and so on.

In this article, we first provide an overview of our necessary basic analytical and bioanalytical methods and their findings that led us to grasp molecular biosensing mechanisms inherent in human erythrocytes for the appreciation of aging and determination of their lifespan, and summarize their roles in physiology, whereby the intrinsic tilting capability of distal (E7) His residues (their bis-histidyl coordination proficiency to the heme iron) and the $\alpha_1-\beta_1$ (and $\alpha_2-\beta_2$) interface of the Hb molecule has major responsibility. Along with these lines of accomplishments and by integrating the most recent state of Hb research, we attempt to form a new mode of Heinz body formation mechanisms, in which built-in sensors in Hb molecule (*i.e.*, bis-histidyl coordination proficiency of distal (E7) His residues and the $\alpha_1-\beta_1$ (and $\alpha_2-\beta_2$) interface) can control degradation of the Hb molecule to hemichrome depending on internal and external conditions in the erythrocyte, and subsequent clustering of Heinz bodies within the erythrocyte. Granting this new mode (molecular sensing) of Heinz body formation mechanisms to be basic premise, we then examine how these new views contribute to deeper understanding of clinical aspects of hemoglobinopathies and hemolytic anemia and its associated acute blood loss, in which the mechanisms for acute hemolytic crisis cannot be explained on the basis of conventional views.

Experimental Accomplishments

Hemichrome formation (Degradation of the Hb molecule to Hemichrome) observed in Human Hb (HbO_2) even at physiological pH and temperature: UV/VIS spectroscopic observations

The dynamics of the reaction of human Hb with O_2 provide them particularly suitable O_2 carriers. In the O_2 binding process of Hb, the iron remains in the ferrous state so that the reaction is an oxygenation, not an oxidation. However, once the molecule is oxygenated, the resultant species (HbO_2) must undergo oxidation by the bound O_2 to

the ferric met-form. If HbO₂ is oxidized (autoxidized), the product (ferric metHb) cannot be oxygenated in its present form.

In this regard, it has been suggested that the autoxidation process of Hb may be associated with transformation of the oxidized molecule (high-spin Fe³⁺) into hemichrome, the formation of which can result in the accumulation of soluble and insoluble hemichromes as well as precipitation [8-13]. Formation of hemichrome is known to be enhanced in separated α and β chains [9,13-17]. So, we deal first the innate molecular instability of Hb, which triggers degradation of the molecule to hemichrome. This process is detected readily through UV/VIS spectroscopic observation during the entire process of autoxidation of human HbO₂ [17].

HbO₂ was prepared from freshly drawn samples of human blood (total, 50–80 mL) obtained from healthy donors. The details can be referred to Sugawara et al. (1993) [35]. The autoxidation of HbO₂ was measured by UV/VIS spectroscopic means in 0.1 M buffer over a wide pH range (5.3–10.5) at 37°C. Two milliliters of solution containing 0.2 M buffer was placed in a test tube and incubated in a water bath maintained at 37 ± 0.1°C using a NESLAB temperature control system (Model RTE-100 or 111 or 210; NESLAB Instruments, Inc., Portsmouth, NH, USA). The reaction was started by adding the same volume of fresh HbO₂ solution (50–125 μ M in heme contents). The reaction mixture was then quickly transferred to a spectrophotometric cell (Spectrocell, Type Inject-A-Cell; Funakoshi Co., Tokyo, Japan) with a screwcap stopper. Changes in absorption at 450–650 nm were recorded on the same chart at measured time intervals. Spectra were recorded using an UV/VIS spectrophotometer (JASCO, Model Ubest-50 or V-560 or V-570; Japan Spectroscopic Co., Tokyo, Japan), equipped with a thermostatically controlled (within ± 0.1°C) cell holder. At the final state of each run, Hb molecules were all completely converted to the ferric met form by addition of potassium ferricyanide. The buffers used were: acetate for pH 4.5–5.5, 2-(*N*-morpholino) ethanesulfonic acid monohydrate (MES) for pH 5.0–6.75, *N*-2-hydroxyethylpiperazine-*N'*-2-ethanesulfonic acid (HEPES) for pH 6.55–8.3, 2-(cyclohexylamino) ethanesulfonic acid (CHES) for pH 8.2–10.2, and 3-cyclohexylaminopropanesulfonic acid for pH 10.0–10.5.

Figure 1 indicates how autoxidation is inseparably related to the instability of the Hb molecule and its degradation to hemichrome. Figure 1a shows the spectrophotometric changes over time from 450 nm to 650 nm when fresh HbO₂ was placed in 0.1 M MES buffer (pH 5.0) at 37°C. HbO₂ was autoxidized to its ferric met form (metHb) without showing any hemichrome formation during the entire process. Contrary to this, the situations demonstrated in Figures 1b-1d are very different. Figure 1b illustrates the observed UV/VIS spectra with time for hemichrome formation during autoxidation of HbO₂ when HbO₂ was incubated in 0.1 M MES buffer (pH 6.5) at 40°C. HbO₂ was autoxidized to its ferric met form. However, sudden disruption of the spectra was observed during the late stage of the reaction whereby hemichrome formation could be detected by elevation of the baseline and a shift in isosbestic points caused by precipitation. Similarly it took place at the intermediate stage in 0.1 M HEPES buffer (pH 8.0) at 40°C in the case of Figure 1c, while at the initial stage in the case of Figure 1d in which immediately after fresh HbO₂ was transferred to the cuvette in 0.1 M HEPES buffer (pH 7.0) at 45°C.

In brief, occurrence of pH- and temperature-dependent hemichrome formation could be readily detected in HbO₂ at every stage during the course of autoxidation (*i.e.*, during the initial, intermediate, and final stages) while varying the temperature of the solution from

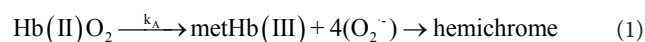
35°C to 55°C and the pH from 4.5 to 10.5. In Figure 2a, we therefore attempted to categorize the phenomenon into the following four cases in terms of $[\text{HbO}_2]_{t=E.P.}/[\text{HbO}_2]_0$, as its emergence was a function of not only the pH and temperature of the solution, but also of the progress of the autoxidation of HbO₂:

- (1) $t = 0$ or $[\text{HbO}_2]_{t=E.P.}/[\text{HbO}_2]_0 = 1 \leq t_{E.P.} < [\text{HbO}_2]_{t=E.P.}/[\text{HbO}_2]_0 = 0.75$;
- (2) $[\text{HbO}_2]_{t=E.P.}/[\text{HbO}_2]_0 = 0.75 \leq t_{E.P.} < [\text{HbO}_2]_{t=E.P.}/[\text{HbO}_2]_0 = 0.25$;
- (3) $t_{E.P.} \leq [\text{HbO}_2]_{t=E.P.}/[\text{HbO}_2]_0 = 0.25$;
- (4) no hemichrome formation during the entire process.

Here E.P. is the observed emergence point of hemichrome formation in each run. $[\text{HbO}_2]_{t=E.P.}/[\text{HbO}_2]_0$ is the ratio of HbO₂ concentration after time $t = E.P.$ to that at time $t = 0$ and can be monitored by the absorbance ratio of $(A_t - A_\infty)/(A_0 - A_\infty)$ at 576 nm (α -peak of HbO₂). $[\text{HbO}_2]_{t=E.P.}/[\text{HbO}_2]_0 = 0.5$ represents equal mixtures of HbO₂ and metHb, *i.e.*, the midpoint of the autoxidation reaction. Hence, case (1) means that hemichrome formation was noticeable at the initial stage of autoxidation. Accordingly, case (2) indicates its occurrence at the intermediate stage, and case (3) at the final stage. In Figure 2a, the symbols used correspond to: ● for case (1), ▲ for case (2), △ for case (3) and ○ for case (4). To determine if the phenomenon was represented by case (3) or case (4), the reaction mixture was converted to metHb by the addition of small amounts of ferricyanide and maintained at the given temperature for 2 days to see if hemichrome precipitation occurred. Thus, the findings suggested that human HbO₂ was highly susceptible to hemichrome formation, even under physiological pH and temperature. The broken lines in Figure 2a show that the threshold for this susceptibility in relation to pH and temperature.

On the other hand, Figure 2b manifests that the isolated α (α_{p-MB}) and β (β_{p-MB}) chains might have much higher susceptibilities to hemichrome formation, when compared with the tetrameric parent molecule, and possess individual susceptibility as detailed in their pH-temperature diagrams. Isolation of α and β chains from the parent molecules was made using sodium *p*-hydroxymercuribenzoate (*p*-MB) by a one-column method using carboxymethyl (CM)-cellulose and alternatively by a two-column method (the details of which can be referred to in Sugawara et al. [17]).

Hence, the occurrence of hemichrome of human HbO₂ can be described as follows:



Along with this line, the question may be arisen as to whether the monomeric Mb (MbO₂) have similar propensity of human HbO₂ to hemichrome. Regarding to this issue, a series of experiments using UV/VIS spectroscopic observation for hemichrome emergence (hemichrome emergence tests) were undertaken for monomeric bovine heart MbO₂. At first, these tests were conducted in 0.1 M buffer over the same range of pH (pH 4.5 to 10.5) and temperature (35 to 55°C). However, our attempts failed to recognize any hemichrome emergence in this pH and temperature range. In order to further check this point, we made an attempt to expand our tests to temperature region exceeding 55°C. In this respect, we employed thermal denaturation measurement for MbO₂ using differential scanning calorimetry (DSC). Ultimately we engaged in these tests over a wide temperature range

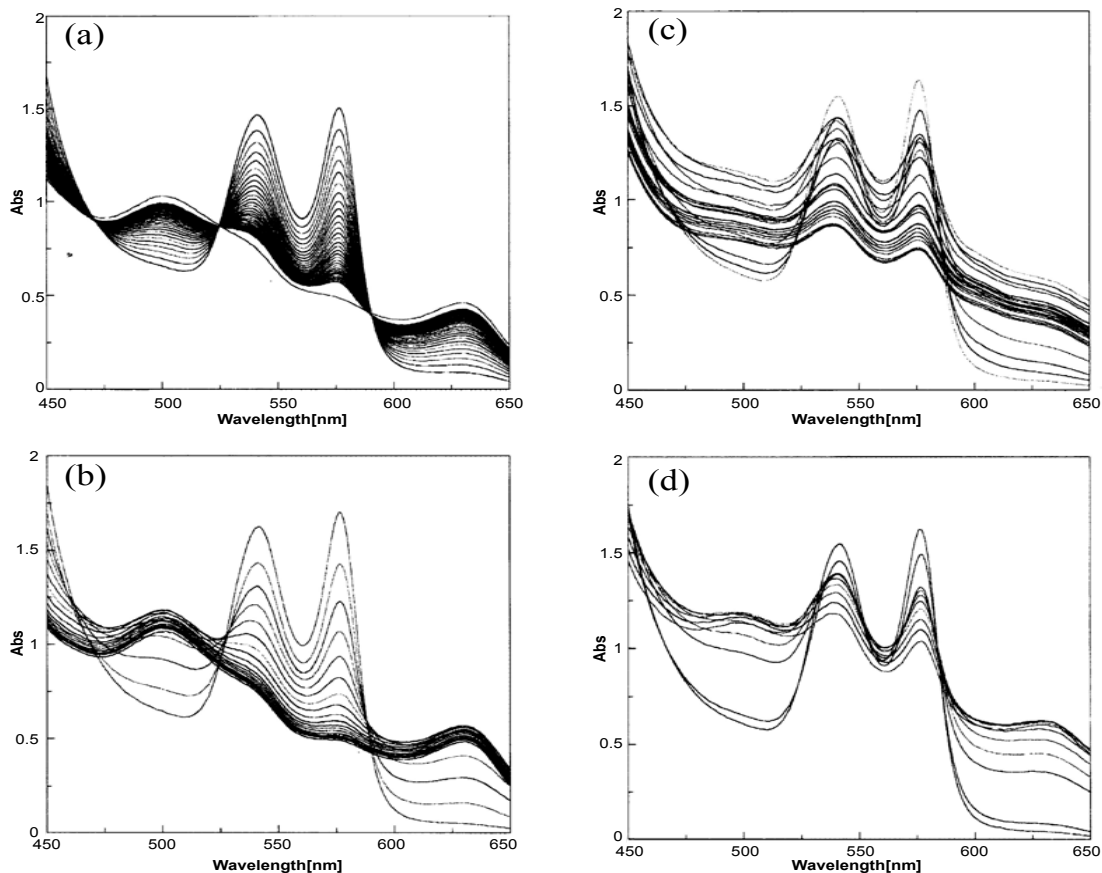


Figure 1: Hemichrome formation associated with human HbO₂ autoxidation, redrawn from Sugawara et al. [17]. UV/VIS spectral changes over time for hemichrome formation associated with human HbO₂ autoxidation in which the reaction was monitored (a) in 0.1 M MES buffer (pH 5.0) at 37°C and scanning interval = 15 min; (b) in 0.1 M MES buffer (pH 6.5) at 40°C and scanning interval = 150 min; (c) in 0.1 M HEPES buffer (pH 8.0) at 40°C and scanning interval = 150 min; (d) in 0.1 M HEPES buffer (pH 7.0) at 45°C and scanning interval = 60 min. Conditions: HbO₂ concentration was 235 μM (in heme contents).

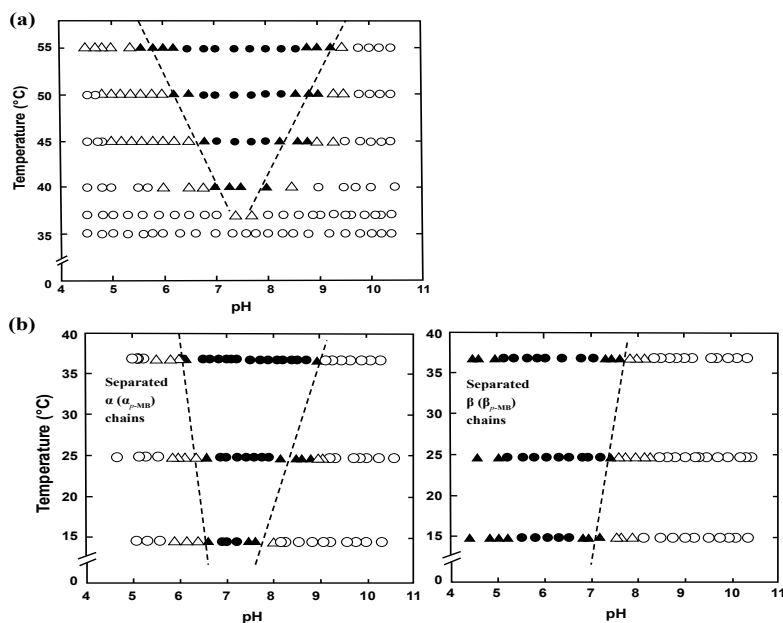


Figure 2: Hemichrome formation associated with human HbO₂ autoxidation. (a) pH-temperature diagram for HbO₂ autoxidation. (b) pH-temperature diagrams for the autoxidation of isolated α and β chains. The symbols used are as follows: ●- hemichrome formation noticeable at the initial stage during the course of autoxidation; ▲- at the intermediate stage; △- at the final stage; ○- autoxidation reaction proceeded with no hemichrome formation during the entire process.

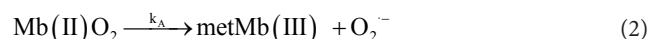
for bovine heart MbO₂ from physiological to temperatures just before thermal unfolding [17].

Mbs (involving MbO₂ and met Mb) were isolated from bovine heart muscle, in which the essential step was chromatographic separation of MbO₂ from metMb on a DEAE-cellulose column. Thermal denaturation of bovine heart Mb was assessed by differential scanning calorimetry in terms of T_d, the temperature at which the transition is half complete. A non-adiabatic calorimeter (DSC, Seiko I & E DSC-10/SSC-570 Thermal Controller Model, Tokyo, Japan) was used at a heating rate of 1°C·min⁻¹ and at protein concentrations of 1.5-5.5 mg·ml⁻¹. After treatment of the raw DSC data, in which correction of the sample curve for changes of slope observed in a run with buffer in each cell was made by subtracting the buffer curve from the protein curve point by point, the linear portions of the corrected curve corresponding to pre- and post-transition base lines were extrapolated to T_d. T_d was also determined by successive area measurements until the vertical line drawn at T_d divided the peak area into two halves. The area under heat capacity curve was determined by means of a planimeter.

Figure 3a is an example of DSC scanning for MbO₂ in 0.1 M HEPES buffer at pH 7.4. In terms of T_d, that is, the temperature at which the thermal unfolding is half complete, Figure 3b gives an upper limit temperature to examine whether hemichrome formation associated with autoxidation can be observed in monomeric MbO₂ or not, although the concentration (0.91 mM) used for DSC measurement was 100 times higher than that of our hemichrome emergence test.

Considering an upper limit temperature in each run, our search for detecting possible hemichrome emergence was carried out by varying pH of the solution from 4.5 to 10.5 and varying the temperature from the physiological level to the level just before thermal unfolding. Typical examples are shown in Figure 3c and 3d, where k_A represents the

observed first-order rate constant of autoxidation of MbO₂ at a given pH and temperature. In air-saturated buffers, MbO₂ is oxidized by the bound O₂ to its ferric met form (metMb) with generation of superoxide anion radical (O₂⁻) as essentially in the same manner as HbO₂:



Here k_A is given by:

$$d[\text{MbO}_2]/dt = k_A \cdot [\text{MbO}_2] \quad (3)$$

In the hemichrome emergence tests, the ratio of MbO₂ concentration after time *t* to that at time *t* = 0 was monitored by absorbance change, for instance, at α-peak (581 nm) of MbO₂. In each run, k_A in hr⁻¹ was determined from the slope of linear plots of -ln([MbO₂]_{*t*}/[MbO₂]₀) versus time and plotted against temperature of the solution in Figure 3c and against the inverse of the absolute temperature, that is Arrhenius plots in Figure 3d. In these figures, our experimental data gave a single straight line against the temperature examined at constant pH of the solution. This implies that there was no hemichrome emergence (formation) under these circumstances. This point was also confirmed by the resulting activation energy, E_A. From the slope of each straight line on Arrhenius plots shown in Figure 3d, E_A was calculated and appeared to be almost constant, i.e., 121.55 ± 14.38 KJ·mol⁻¹ (29.08 ± 3.44 Kcal·mol⁻¹) over the pH range of 4.5 to 10.5 and at the temperature range greater than or equal to 35°C. These were in good agreement with those observed by Goto and Shikama [36], where E_A is almost constant with the value of 26.5 Kcal·mol⁻¹ (110.77 KJ·mol⁻¹) over pH range of 5 to 10 using bovine heart MbO₂ based on the measurements of the rate at 0, 15, 25, and 30°C.

We, therefore, concluded that the monomeric bovine heart Mb (MbO₂) did not show any propensity for hemichrome formation over a wide pH range of 4.5 to 10.5 and over a wide temperature range

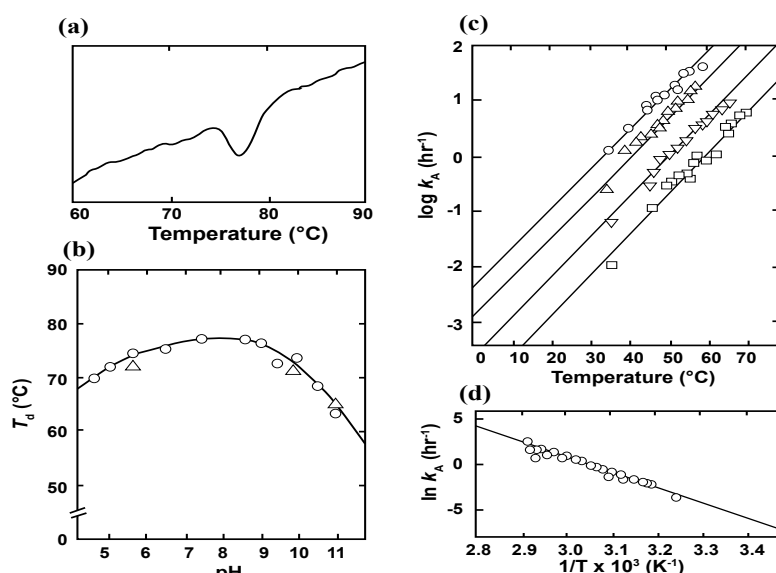


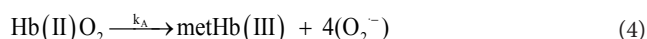
Figure 3: Hemichrome formation test for monomeric bovine heart Mb. (a) Tracing of DSC curve for unfolding of bovine heart MbO₂ in 0.1 M HEPES buffer at pH 7.4. Protein concentration was 2.35 mg·ml⁻¹ (0.91 mM). (b) By means of DSC, the properties of thermal unfolding of bovine heart MbO₂ and metMb were depicted as a function of pH and temperature in terms of T_d (i.e., the temperature at which the transition is half complete). Protein concentration was 1.5 - 5.5 mg·ml⁻¹ (0.91 to 5.81 mM). ○: MbO₂, △: metMb. (c) Temperature dependence of first-order rate constants, k_A of autoxidation of bovine heart MbO₂. The autoxidation was measured in 0.1 M buffer at a given pH and temperature under air saturated condition. The resulting data of pH 5.0 in 0.1 M MES buffer (○), 6.0 in 0.1 M MES buffer (△), 7.0 in 0.1 M HEPES buffer (▽) and 9.0 in 0.1 M CHES buffer (□) were plotted against a given temperature. MbO₂ concentration was 97μM. (d) Arrhenius plot of k_A, measured in 0.1 M HEPES buffer at pH 7.4.

from physiological to temperatures just before thermal unfolding. Contradictorily, higher susceptibilities to hemichrome formation as well as occurrence of hemichrome emergence even under physiological pH and temperature was pronounced to be the most significant feature of the tetrameric human HbO₂ that is O₂-carrying protein in the blood.

Oxidative behavior of human Hb (HbO₂): pH-Dependent biphasic autoxidation curves seen in acidic solutions

Since the early works of Brooks [37,38], the oxidative process (autoxidation) of human Hb has been investigated by several researchers. Among others, Monsouri and Winterhalter [39] and Tomoda et al. [40] observed that the rate of autoxidation was strongly dependent upon the pH values of solutions. The study of Monsouri and Winterhalter [39] also showed that autoxidation of human HbO₂ exhibited a biphasic nature, with an initial fast (k_A^f) reaction followed by a second slower (k_A^s) reaction, when observed in acidic solutions. Following the method of Monsouri and Winterhalter [39], we here focus on the biphasic nature of the autoxidation seen in acidic solutions on the basis of our previous report [35].

As previously shown, Figure 1a is a representative example, in which HbO₂ was autoxidized to its ferric met form through the tendency of the bound O₂ to oxidize ferrous heme iron (II) with generation of superoxide anionradical (O₂⁻), as in the same fashion in MbO₂ autoxidation mentioned above:



Here k_A represents the observed rate constant of the reaction at a given pH and temperature. The reaction process was followed in each experimental run by the ratio ($[\text{HbO}_2]_t/[\text{HbO}_2]_0$) of HbO₂ concentration after time t to that at time $t=0$ that was monitored by the absorbance ratio of $(A_t - A_\infty)/(A_0 - A_\infty)$ at 576 nm (α -peak of HbO₂). The ratio was then plotted against time. Each curve shown in Figure 4a represents the $-\ln([\text{HbO}_2]_t/[\text{HbO}_2]_0)$ versus time plot (first-order plot) for this phenomenon. In acidic-to-neutral solutions, the reaction was biphasic and can be described by first-order kinetics containing two rate constants as follows:

$$d[\text{HbO}_2]/dt = P \cdot \exp(-k_A^f t) + (1-P) \cdot \exp(-k_A^s t) \quad (5)$$

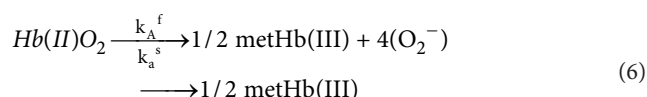
This equation was originally proposed by Monsouri and Winterhalter [39], where k_A^f and k_A^s represent first-order rate constants for the initial fast oxidation and the second slower oxidation, respectively, and P is the molar fraction of the initial fast component. In the Figure, solid lines represent the best fitting derived by the least-squares method using the equation to each run. However, when the pH of solutions is more than 8, a plot of $-\ln([\text{HbO}_2]_t/[\text{HbO}_2]_0)$ versus time showed a single-phase reaction with a single first-order rate constant, although curve fittings could be made using the same equation under conditions setting $P=0.5$ and $k_A^f = k_A^s$. Thus, it was shown that the biphasic behavior seen in acidic solutions gradually disappeared with increasing pH of solutions and completely disappeared if the pH of solutions was more than 8.

In this way, the kinetic parameters and molar fraction of the initial fast component (P) for the biphasic nature of human HbO₂ autoxidation were established in each run in 0.1 M buffer at 37°C (Table 1). It was evident that the values of P varied from 0.47 to 0.53. This means that HbO₂ was autoxidized with half of the component via the reaction process with the initial fast reaction with k_A^f and the

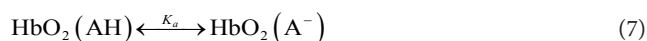
pH	P	k_A^f (h ⁻¹)	k_A^s (h ⁻¹)	k_A^s/k_A^f
5.3	0.47	0.438	0.078	0.178
5.9	0.48	0.270	0.030	0.111
6.2	0.48	0.134	0.0154	0.115
6.55	0.49	0.070	0.010	0.142
6.9	0.53	0.0465	0.0073	0.157
9.15	0.50	0.0095	0.0095	1.0
9.5	0.50	0.0184	0.0184	1.0
9.7	0.50	0.0381	0.0381	1.0
10.2	0.50	0.080	0.080	1.0
10.4	0.50	0.157	0.157	1.0

Table 1: Summary of kinetic parameters for the autoxidation of human HbO₂ in 0.1 M buffer obtained by least-squares fitting to the experimental data in each run, redrawn from Sugawara et al. [34].

other half via the procedure with the second slower rate (k_A^s). Thus, autoxidation of human HbO₂ may be written as follows:



To clarify the processes behind this phenomenon, the obtained values of k_A^s/k_A^f were plotted against the pH of solutions (Figure 4b). In the Figure, the solid line shows that the computed curve obtained by the least-squares method fitted the experimental data over the whole range of pH 5-10.5, where a single dissociable group, AH with K_a , was assumed to be involved in the reaction:



For neutral amino acids, acid-base equilibrium is usually given by the dissociation constant: $\text{AH} \leftrightarrow \text{A}^- + \text{H}^+$ and thus $K_a = [\text{A}^-] \cdot [\text{H}^+]/[\text{AH}]$. The best fitting was achieved when $\text{p}K_a = 7.4$ (at 37°C). In this regard, Hermans and Rialdi [41,42] reported microcalorimetric ionization data on amino-acid residues for sperm whale myoglobin (Mb) in which they assigned the His residue with values of $\text{p}K_a = 6.62$, the standard Gibbs energy (ΔG°) = 37.7 kJ·mol⁻¹, the enthalpy (ΔH) = 29.7 kJ·mol⁻¹, and the entropy (ΔS°) = -26.8 J·mol⁻¹·K⁻¹. It is unwise to identify a dissociation group only by its $\text{p}K_a$ value because of the anomalies often found in proteins. Hence, we confirmed that AH must be a His residue assuming that the primary and tertiary structures of α and β subunits are remarkably similar to each other and to Mb. This fact provides information for the existence of a pH-sensed molecular device that can manifest the biphasic autoxidation of the HbO₂ tetramer via participation of a single amino-acid residue with $\text{p}K_a = 7.4$ (at 37°C).

In order to not only elucidate the biphasic characteristics of human HbO₂ autoxidation but also to clarify how the Hb molecule can prompt the range of fast (k_A^f) and slow (k_A^s) components against pH values of the solutions, chain separation of the constituted chains from the parent molecules and rate measurements for the separated chains were conducted. Chain separation was made using p-MB [17], as mentioned above.

Figure 5 shows the obtained pH profiles for the autoxidation rate of the isolated $\alpha_{\text{p-MB}}$ and $\beta_{\text{p-MB}}$ chains. With reference to the rates (k_A^f and k_A^s) of the parent molecules calculated from biphasic autoxidation curves, the isolated chains were shown to be oxidized much more

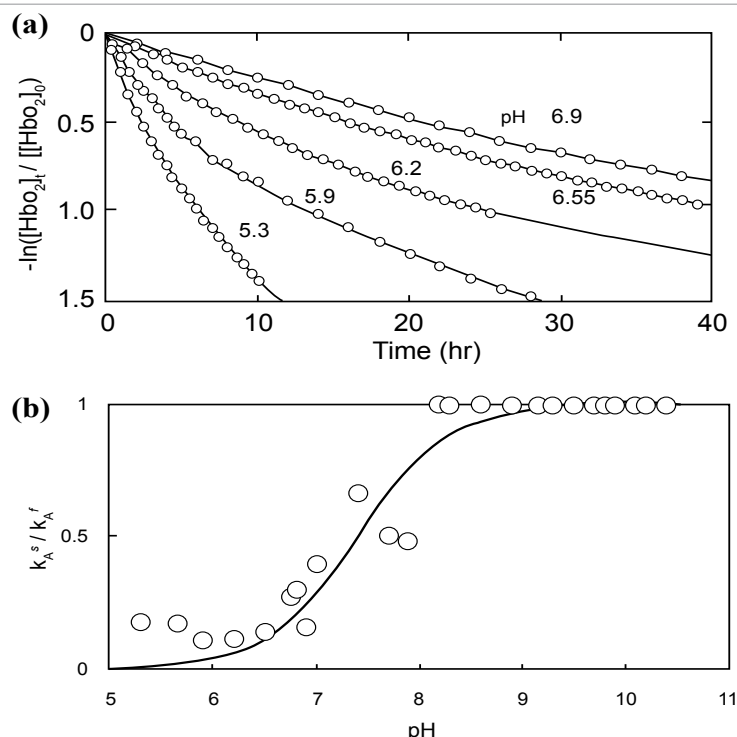


Figure 4: Oxidative behavior of human Hb (HbO₂) in various buffer conditions. (a) A $-\ln([HbO_2]_t/[HbO_2]_0)$ versus time plot (first-order plot) for human HbO₂ autoxidation. Two-phase autoxidation with an initial fast reaction (k_A^f) followed by a second slower reaction (k_A^s) seen in acidic-to-neutral pH ranges. Solid lines represent the least-squares fitting to experimental data in each run. Conditions: HbO₂ concentration was 50–125 μ M (in heme contents); and the reaction proceeded in 0.1 M buffer at 37°C. (b) A k_A^s/k_A^f versus pH plot for human HbO₂ autoxidation. The solid line stands for the best-suited fitting under the assumption that a single, dissociable group, AH with K_A , can be involved in the reaction. This was achieved with the setting $pK_A = 7.4$.

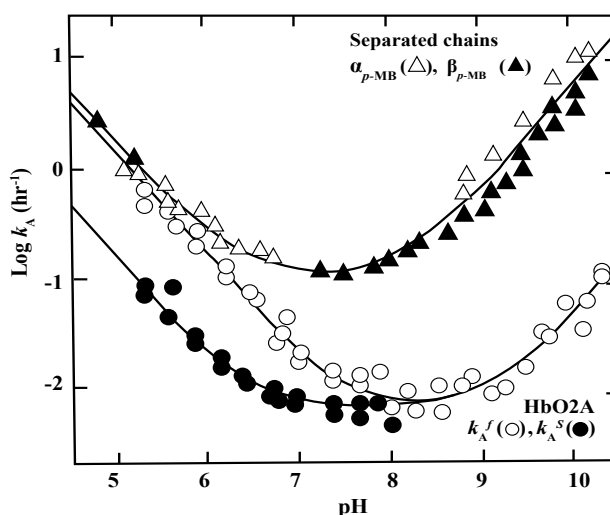
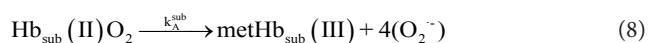


Figure 5: Logarithmic values of first-order rate versus pH plot for autoxidation of the isolated α (α_{p-MB}) and β (β_{p-MB}) chains with a reference to the relevant values (k_A^f and k_A^s) of the parent molecules, redrawn from Sugawara et al. [34]. Conditions: the concentration of isolated α and β chains was 50 μ M (in heme contents); the reaction rate was measured in 0.1 M buffer at 37°C.

rapidly to the ferric met-form over the entire pH range (5-10.5) because the reaction followed simple, first-order kinetics as follows:



Where Hb_{sub} represents each subunit of the Hb molecule. It was also shown that the rate of the initial first component (k_A^f) of the parent

molecules was found to lie closer to the values of k_A for the isolated α_{p-MB} and β_{p-MB} chains if the pH of solutions was less than 6. Similar pH profiles were obtained for p -MB-removed chains, *i.e.*, the α_{SH} and β_{SH} chains. p -MB can be removed from the α_{p-MB} and β_{p-MB} chains by incubation with 2-mercaptoethanol, as described elsewhere [30]. In separated-chain solutions, the protein is known to exist in equilibrium

of $\alpha \leftrightarrow \alpha_2$ or $\beta \leftrightarrow \beta_4$, respectively. Under our experimental conditions, the monomeric form (87%) was present in the separated α chain, whereas the tetrameric form (99%) was predominant in the β chain. This estimation was made on the basis of the results by McDonald et al. [16]. Accordingly it became evident that the isolated α and β chains could be oxidized much more readily over the measured pH range (5–10.5) when compared with the respective rates of the parent molecules as a reference. With respect to the difference in the rate between the isolated individual chains, this seemed to be within reasonable experimental errors in the values of α_{p-MB} and β_{p-MB} chains, and the α_{SH} and β_{SH} chains.

Thus, the obtained findings put forward an idea that the individual chains have acquired considerable resistance to oxyheme autoxidation in their tetrameric protein architecture. The same appears to be the case in which human HbO₂ has acquired a pH-sensitive molecular device, whereby participation of a single dissociation group of amino-acid residue (probably a His residue) with $pK_a=7.4$ (at 37°C) plays a key role, as a consequence of development of the tetrameric protein architecture. We will see later that this issue was the starting point that led us to uncover a new mode of subunit interaction of the Hb molecule that can be emerged from participation of the $\alpha_1-\beta_1$ (and $\alpha_2-\beta_2$) interface via distal side perturbations within the heme pocket relying upon inherent tilting capability of the distal (E7) His residues (i.e., $\alpha 58\text{His}$ (E7) in the α chain and $\beta 63\text{His}$ (E7) in the β chain).

We must be careful when evaluating the data of the isolated chains shown in Figure 5. Because of the instability of Hb molecules and their relationship to hemichrome, the first-order rate constant for the isolated chains was established in each experimental run using only the initial slope of the $-\ln([\text{Hb}_{\text{sub}}\text{O}_2]_t/[\text{Hb}_{\text{sub}}\text{O}_2]_0)$ versus time plot. Once hemichrome precipitation arose, one could not get the endpoint spectrum (the ferric met form) of the reaction, whereby Hb molecules in the reaction mixture should be all completely converted to the ferric met form by addition of potassium ferricyanide. Hence, measurement must be confined within the initial range, in which existence of isobestic points of the spectra that means non-occurrence of hemichrome formation during the entire reaction process was surely guaranteed.

Hemichrome emergence and subsequent formation of heinz bodies within erythrocytes: observation in normal human erythrocytes during mild heating

Herein we consider the results of our study investigating the formation of Heinz bodies in normal human erythrocytes [32-34]. Aliquots of freshly drawn venous blood from healthy donors were subjected to mild heating at desired temperature above 37°C for 30 min to investigate hemichrome formation and subsequent Heinz-body formation in normal human erythrocytes. Heinz bodies were then visualized by exposing blood smears to acetylphenylhydrazine and staining with crystal violet. Changes within the erythrocytes were observed using light microscopy under oil immersion.

Prior to the acetylphenylhydrazine test [42,43], blood samples were subjected to mild heating *in vitro*. A 2-mL sample was placed in a test tube and incubated in a water bath maintained at each desired temperature ($\pm 0.1^\circ\text{C}$) above 37°C for 30 min using a NESLAB temperature control system (Model RTE-100 or 111 or 210 or 221). In each experimental run, we employed a temperature-untreated reference as a control. The blood sample used as a temperature-

untreated reference was kept at a low temperature (0–4°C) for as long as possible after withdrawal from the donor, and never exposed to temperatures above room temperature.

β -Acetylphenylhydrazine and crystal violet (research grade for pathology) were used (Wako Pure Chemical, Co., Osaka, Japan) for the procedure, as described by Bauer [43]. A 0.1-mL aliquot of blood sample was suspended in 2 mL of acetylphenylhydrazine solution, in which 100 mg of acetylphenylhydrazine and 200 mg of glucose in 100 mL of 0.067 M phosphate buffer were dissolved at pH 7.6. Using a “blowout” pipette, the solution was aerated twice or thrice by drawing it up into the pipette and blowing it out, together with a small quantity of air. This mixture was incubated at 37°C for 2 h. Aeration was repeated halfway through and immediately after the 2-h incubation. A drop (approximately 10 μL) of the resulting mixture was placed on a coverslip, which was then inverted onto a microscope slide containing 30 μL of crystal violet solution. The smear was allowed to stand for 20 min in wet preparation at room temperature and subsequently examined under a light microscope (Nikon Model-FXA; Nikon Co., Tokyo, Japan) equipped with a digital camera (Olympus Model-DP-70; Olympus Co., Tokyo, Japan). Photomicrographs were taken under oil immersion at 1,000 \times magnification. Subsequently, the number of Heinz bodies per cell was counted in 100 red cells per view.

Figure 6 shows representative images of Heinz bodies within normal red corpuscles (obtained from a healthy donor) during mild heating to a given temperature with using a temperature-untreated reference as a control. Heinz bodies were observed in each smear. Figure 7 puts on view about an entire image of changes of the number of the Heinz bodies per cell in each smear. Here histograms of samples treated at 37°C, 40°C, 42°C and 45°C are displayed with a temperature-untreated sample as a reference based on the number of Heinz bodies contained in each of 100 red cells per view. These results confirmed that Heinz-body formation increased with increasing temperature of blood samples treated at temperatures more than 37°C. Red cells in blood samples exposed to 48°C were hemolyzed. Some of the changes are also shown in Figure 8a; histograms of the samples treated at 37°C and 42°C are laid out with a temperature-untreated sample as a reference.

The other histograms shown in Figure 8b-8f represent the results from another five healthy donors, with a temperature-untreated sample as a reference. Although there was considerable inter-individual variation, temperature-dependent Heinz-body formation was apparent in all preparations. Arithmetic summation was used for all histograms to reduce variability and allow better assessment of temperature-dependent Heinz-body formation. The results of this summation are shown in Figure 9. Solid lines represent the curves derived using the least-squares method using a Gaussian curve. Each computed curve showed satisfactory-to-good agreement with the experimental data over the entire range. The following is a summary of the Gaussian constants resulting from the least-squares fitting: a (peak height) = 101, b (peak width at half of maximum) = 5.0 and c (peak location) = 4.0 for blood samples treated at 42°C; a=215, b=3.5 and c=1.0 for blood samples treated at 37°C; and a=215, b=3.0 and c=0.8 for temperature-untreated blood samples.

***In vitro* evaluation of blood fluidity during mild heating using a micro-channel array flow analyzer (MC-FAN) to provide an index of erythrocyte deformability**

In 1992, Kikuchi et al. (1992) described a tool for measuring

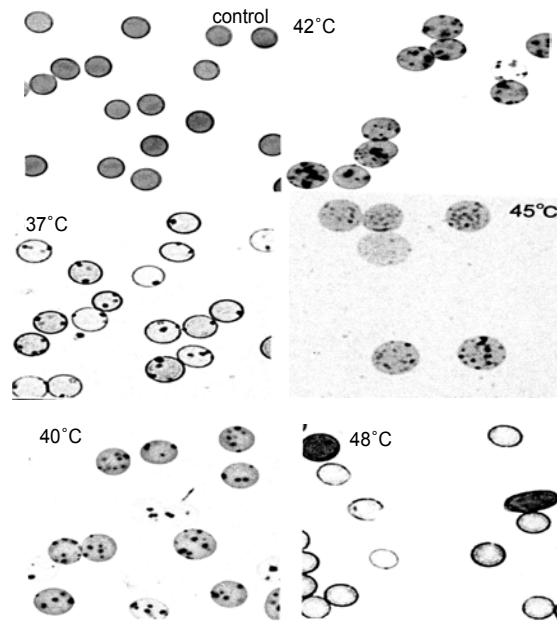


Figure 6: Microscopic views of Heinz bodies after mild heating of blood samples obtained from one healthy donor, redrawn from Sugawara et al. [32]. Using a temperature-untreated sample as a control, aliquots of freshly drawn venous blood were subjected to mild heating at 37°C, 40°C, 42°C, 45°C and 48°C for 30 min. Heinz bodies were then visualized by exposure to acetylphenylhydrazine and dyeing with crystal violet. The changes that occurred within erythrocytes were observed by light microscopy under oil immersion.

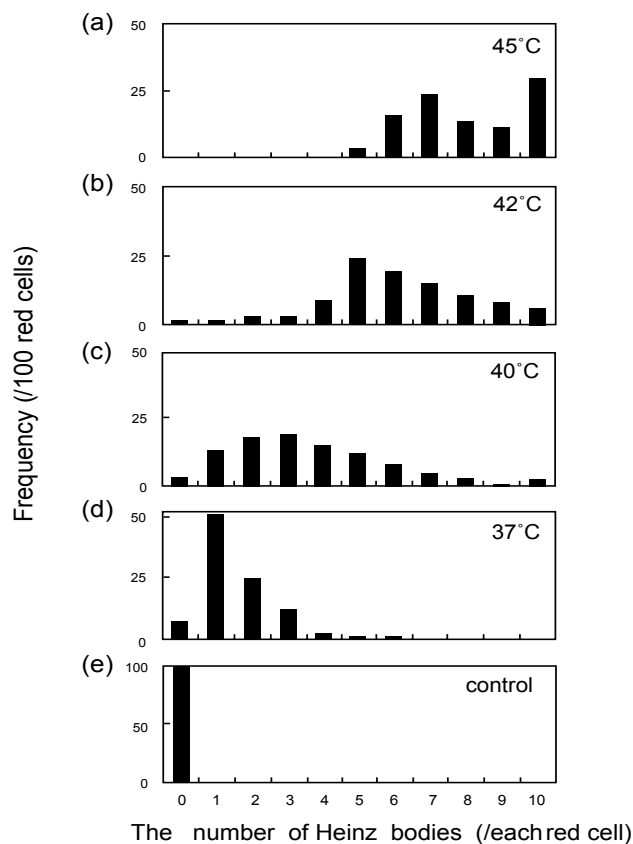


Figure 7: Histograms obtained from the microscopic views as shown in Figure 6, redrawn from Sugawara et al. [32]. On the basis of the number of Heinz bodies contained in each of 100 red cells per view, samples treated at (a) 45°C, (b) 42°C, (c) 40°C and (d) 37°C are displayed with a temperature-untreated sample as a reference (e). The results demonstrate that hemichrome emergence and subsequent formation of Heinz bodies within the erythrocytes increased with increasing temperature treated of blood samples over 37°C.

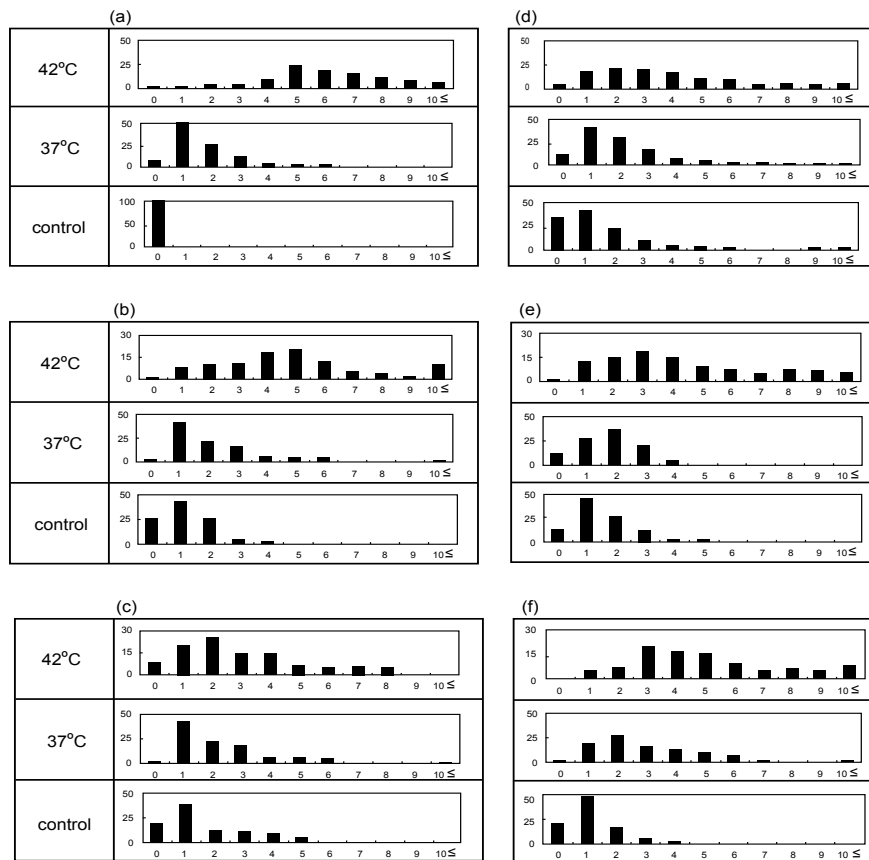


Figure 8: Histograms representing Heinz bodies detected in blood samples after mild heating at $>37^{\circ}\text{C}$, redrawn from Sugawara et al. [32]. The histograms for 37°C and 42°C are displayed using a temperature-untreated sample as a reference. One-hundred red cells were chosen, and the number of Heinz bodies contained in each red cell counted. (a) was constructed from the microscopic views (Figure 6) and the concerned histograms shown in Figure 7, whereas (b–f) represent the results from another five healthy donors.

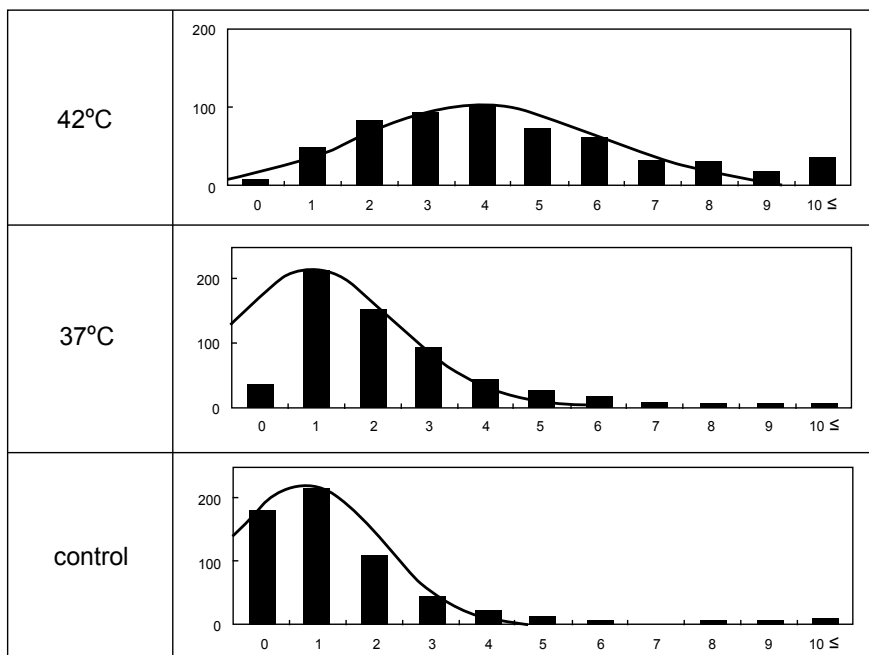


Figure 9: Histograms obtained from the arithmetic summation of all histograms shown in Figure 8, redrawn from Sugawara et al. [32]. The solid lines show the computed curve obtained by the least-squares method using a Gaussian curve. The resulting Gaussian constants are summarized in the text.

the fluidity or rheology of blood [45]. This has subsequently been implemented in numerous studies [45-52]. A MC-FAN includes a characteristic V-shaped groove array in an integral circuit with 8,736 flow paths (width, 7 μm ; length, 30 μm ; depth, 4.5 μm) engraved on a 15 \times 15 \times 0.5-mm single-crystal silicon substrate using an anisotropic etching technique. The array is housed in a cylinder. This equipment enables observation of red cells passing through individual micro-channel arrays by use of an inverted metallographic microscope, as well as to evaluate blood fluidity through the groove array in terms of the transit time of the blood sample for a given transit sample volume. Flow rate can be determined by timing when the meniscus of the blood sample crosses graduation marks at 10- μL intervals from 0 μL to 100 μL . The transit sample volume is therefore equivalent to the loss of the blood sample within the cylinder. Here we look into our *in vitro* findings on blood fluidity during mild heating using a MC-FAN (HR300; Hitachi Haramachi Electronics Co., Ibaraki, Japan) [32,33].

Donors were male or female student volunteers from the Prefectural University of Hiroshima (Hiroshima, Japan) and were aged 18-22 years. All volunteers were aware of the aims and procedures of the study. They gave their written informed consent to participate. The study protocol was approved by the Ethical Review Board of the Prefectural University of Hiroshima. Nine aliquots of samples of freshly drawn venous blood (10 mL in total) were obtained from healthy donors and mixed with one aliquot of 3.2% sodium citrate ($\text{Na}_3\text{C}_6\text{H}_5\text{O}_7 \cdot 2\text{H}_2\text{O}$) or 3.8% sodium citrate ($\text{Na}_3\text{C}_6\text{H}_5\text{O}_7 \cdot 5\text{H}_2\text{O}$). Blood samples were centrifuged at 400 \times g for 10 min at 0-4 $^\circ\text{C}$ to eliminate the possibility of interference with blood fluidity measurements caused by platelet aggregation onto micro-channel flow paths. The supernatant (platelet-rich plasma (PRP)) was

then discarded using a narrow Teflon-lined capillary connected to a waterjet pump. The remainder (PRP-removed blood) was subjected to mild heating prior to application to the MC-FAN. A 2-mL aliquot was placed in a test tube and incubated in a water bath maintained at each desired temperature ($\pm 0.1^\circ\text{C}$) above 37 $^\circ\text{C}$ for 30 min using a NESLAB temperature control system (Model RTE-100 or 111 or 210 or 221).

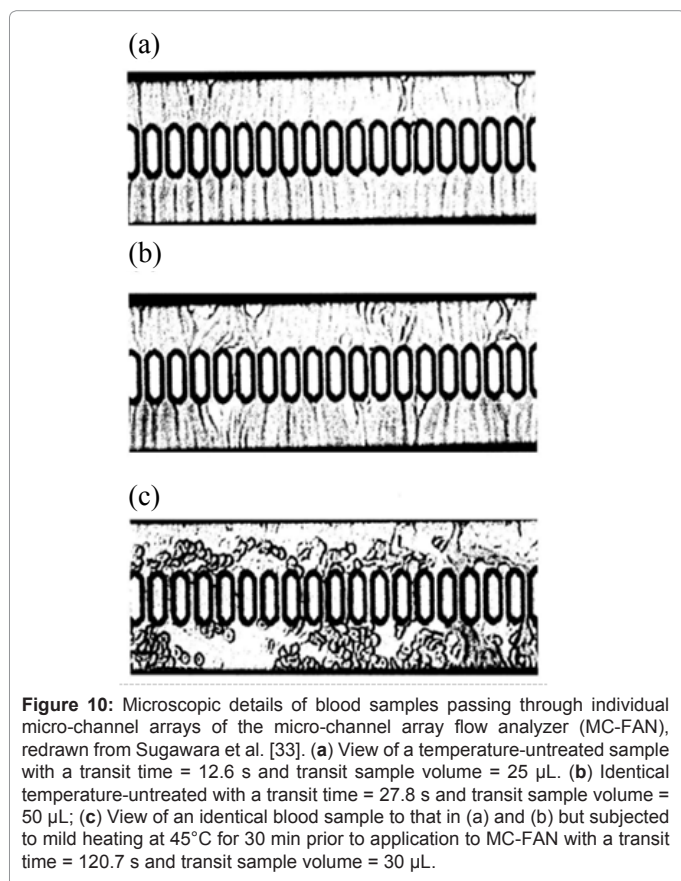
Using a 1-mL disposable syringe and a thin catheter, 200 μL of each temperature-treated blood sample were introduced into a groove array via the cylinder house, which was connected to the inlet hole. The sample was allowed to flow through the cylinder house by applying a pressure difference of 20 cm H_2O . Red cells passing through individual micro-channel arrays were monitored using an inverted metallographic microscope, a video camera, and a video-recorder system. As shown in Figure 10a and 10b, microscopic images revealed good erythrocyte deformability in temperature-untreated samples subjected to MC-FAN. However, a marked decline in erythrocyte deformability was observed in blood samples treated at temperatures greater than 37 $^\circ\text{C}$ for 30 min. An example is shown in Figure 10c. Temperature-treated samples also demonstrated increased transit time for low transit sample volumes.

Figure 11 illustrates some examples of blood fluidity of temperature-treated samples measured as transit time versus transit sample volume. These graphs show that erythrocyte deformability decreased with increasing temperature at temperatures above 37 $^\circ\text{C}$, although there was considerable inter-individual variation. Blood was therefore obtained from a further six healthy donors, and temperature-treated samples compared with a temperature-untreated sample as a reference. The results were similar to those in Figure 11. Both sets of results ($n=10$) are summarized in Table 2. The temperature-dependent decrease in erythrocyte deformability induced by mild heating was evaluated using the Student's *t*-test on the total sum of the difference in transit times between a given temperature-treated sample and each temperature-untreated reference, with varying transit sample volumes (20, 40 and 60 μL). Significant differences ($p < 0.001$) between treated and control samples were evident for all samples treated at 45 $^\circ\text{C}$ with transit sample volumes of 20, 40 and 60 μL , and all samples treated at 42 $^\circ\text{C}$ with transit sample volumes of 20, 40 and 60 μL . To adequately show the results of Figure 11, significant differences ($p < 0.001$) of the samples treated at 45 $^\circ\text{C}$ (*i.e.*, two-point lines) and 42 $^\circ\text{C}$ (*i.e.*, one-point lines) against the control samples (*i.e.*, solid lines) are shown. Furthermore a triplicate-experiment was conducted for each of three healthy donors ($n=3$) in terms of transit time *versus* transit sample volume, whereby blood fluidity was assessed by the measurements each being allowed an interval of two to three months (Figure 12). On the basis of these findings, we concluded that erythrocyte deformability decreased with increasing temperature of blood samples treated at temperatures more than 37 $^\circ\text{C}$.

New Mode of Molecular Biosensing Mechanisms Inherent in Human Erythrocytes for Appreciation of Cell Aging and Determination of their Lifespan

Human red blood corpuscles survive in the circulation for an average of 120 days. Removal of aged and damaged red cells from the blood circulation is essential for its homeostasis. This prompts the question: how do human erythrocytes appreciate aging and determine their lifespan?

Through a series of studies described in the preceding section, we drew seven main conclusions. First, autoxidation of human HbO_2 (the



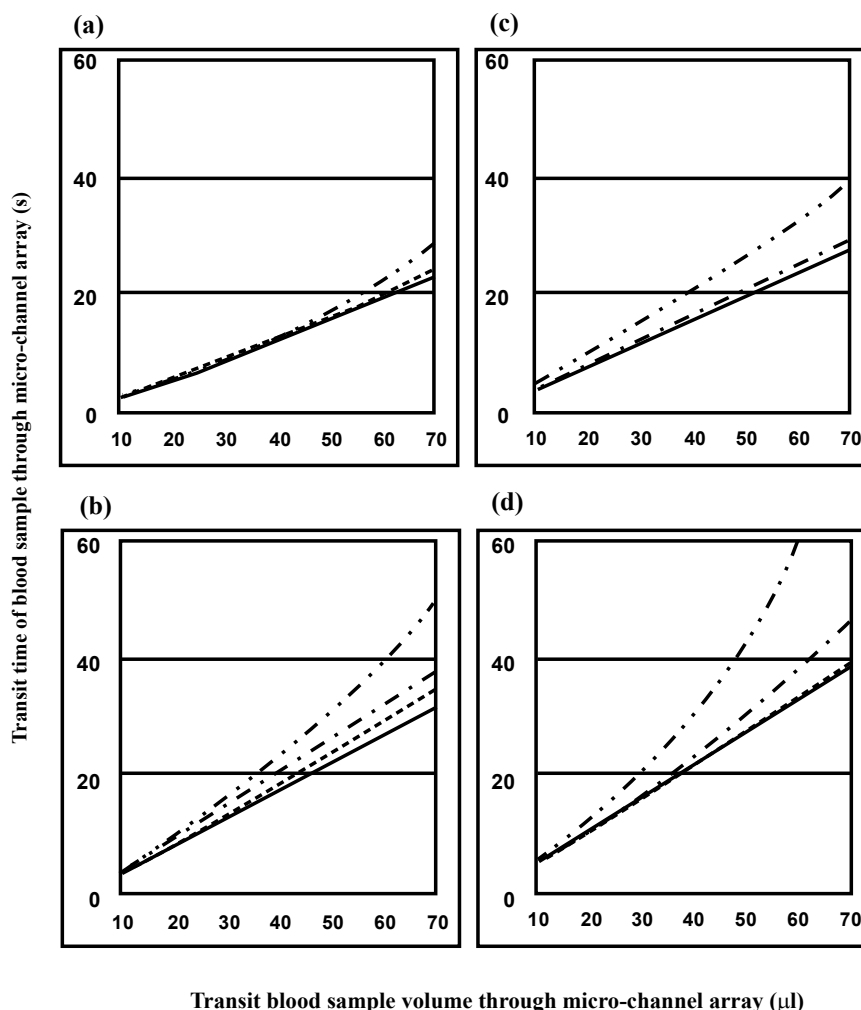


Figure 11: Representative examples ($n = 4$) of blood fluidity measured in terms of transit time against transit sample volume, redrawn from Sugawara et al. [33]. Solid lines represent the temperature-untreated control; broken lines represent samples treated at 37°C; one-point lines represent samples treated at 42°C; two-point lines represent samples treated at 45°C.

	Transit blood sample volume (μL)		
	20 μL	40 μL	60 μL
Temperature-untreated reference	8.0 ± 1.08	16.3 ± 2.24	25.1 ± 3.50
Temperature-treated at 37 °C	7.8 ± 1.35	16.4 ± 2.57	26.4 ± 3.42
Temperature-treated at 42 °C	$8.5 \pm 1.38^{**}$	$18.3 \pm 2.94^{**}$	$36.3 \pm 6.32^{**}$
Temperature-treated at 45 °C	$9.3 \pm 2.46^{**}$	$21.2 \pm 5.99^{**}$	$41.8 \pm 13.23^{**}$

Table 2: Summary of the mean \pm standard deviation of transit time of blood samples (s) for a given transit sample volume (μL), redrawn from Sugawara et al. [33]. Prior to application to MC-FAN, blood samples were subjected to mild heating at 37°C, 42°C and 45°C for 30 min, respectively. The number of subjects was 10. Significant differences ($p < 0.001$) of the temperature-treated samples against the temperature-untreated reference were shown as **.

reaction of which is inevitable in nature for all O_2 -binding proteins and which has been dealt with in the periphery of Hb research) seemed to be inseparably related to the instability of the Hb molecule and its degradation to hemichrome. Second, in terms of pH- and temperature-dependent hemichrome emergence observed by UV/VIS spectroscopy, HbO_2 was supposed to be highly susceptible to hemichrome formation (even under physiological pH and temperature). Third, in contrast to the tetrameric human HbO_2 as O_2 -carrying protein in the blood, the

monomeric bovine heart Mb (MbO_2) did not show any propensity for hemichrome formation over a wide pH range of 4.5 to 10.5 and over a wide temperature range from physiological to temperatures just before thermal unfolding. Fourth, in terms of pH-dependent biphasic autoxidation (k_A^f for the initial fast oxidation and k_A^s for the second oxidation) seen in acidic solutions, participation of a single dissociation group of an amino-acid residue (probably a His residue) with $\text{pK}_a = 7.4$ (at 37°C) appeared to have a key role in how the Hb

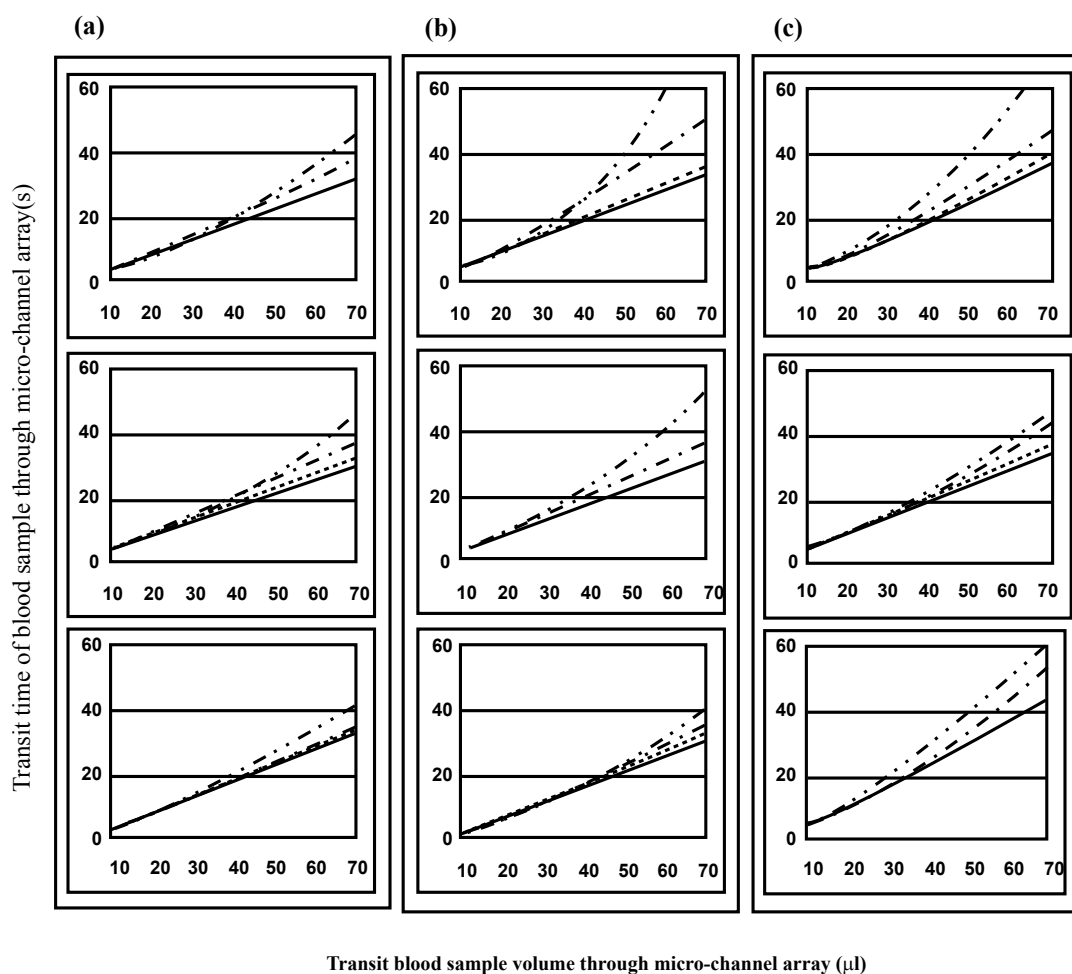


Figure 12: Transit time *versus* transit sample volume plots obtained by a triplicate experiment. Blood fluidity was measured in three stages concerning three healthy donors ((a); (b); (c)), an interval of two to three months being allowed between measurements. Solid lines represent the temperature-untreated control; broken lines represent samples treated at 37°C; one-point lines represent samples treated at 42°C; two-point lines represent samples treated at 45°C.

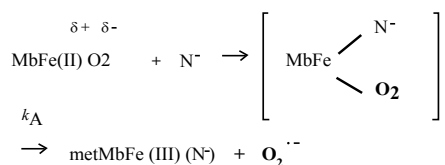
molecule can prompt the range of fast (k_A^f) and slow (k_A^s) components against the pH values of the solutions. Fifth, the isolated α and β chains were oxidized much more readily over the measured pH range (5–10.5) when compared with the respective rates of the parent molecules used as a reference. Sixth, using freshly drawn venous blood from healthy donors, exposure of red cells to acetylphenylhydrazine and subsequent staining with crystal violet revealed a greater abundance of Heinz bodies with increasing temperature if blood samples were subjected to mild heating at temperatures greater than 37 °C for 30 min. Finally, *in vitro* evaluation of blood fluidity during mild heating using a MC-FAN demonstrated a marked decline in erythrocyte deformability with increasing temperature of blood samples if treated at temperatures more than 37°C for 30 min.

In this section, we start to deal with the oxidative behavior (autoxidation) of the human HbO₂ molecule. This is because autoxidation is inseparably related to the instability of the molecule and its degradation to hemichrome, relying upon the intrinsic tilting capability of the distal (E7) His residues (their bis-histidyl coordination proficiency to the heme iron). In Hb research, understanding of subunit interaction between the four Hb chains (how these explain cooperative

O₂ binding) has been the primary focus [22-28]. Most of the emphasis is based on the distinct differences between deoxygenated and oxygenated quaternary structures as determined by X-ray diffraction [23-28]. The configuration of the residues lining the distal side of the heme pocket (where O₂ binds and where geographical alteration can be made by oxygenation) is thought to play a part in controlling access of the ligand to the heme pocket. Nevertheless, the possibility of subunit interactions originating from or being transmitted via distal effects has (for the most part) been neglected [29]. Relatively little attention has been paid to the autoxidation of HbO₂ (oxidation of ferrous heme iron by bound O₂), even though autoxidation is inevitable in nature for all O₂-binding heme proteins. It has been customary to deal with the “periphery” in Hb research.

Shikama [54-58] evaluated various mechanisms proposed for autoxidation involving MbO₂ and HbO₂. He demonstrated clearly that the autoxidation reaction does not simply involve the dissociative loss of O₂⁻ from HbO₂, but is instead caused by the nucleophilic displacement of O₂⁻ from HbO₂ by a water molecule or a hydroxyl ion that enters the heme pocket from the surrounding solvent. The iron is thus converted to the ferric met form, and the water molecule or hydroxyl ion remains

bound to Fe(III) at the sixth coordinate position to form the aqua- or hydroxide-met species. A generalized pathway for this S_N2 mechanism can be written using Mb (MbO_2) as an example:



Here, k_A represents the rate constant of anion-induced autoxidation with nucleophilic anion displacement. N^- can be SCN^- , F^- , OCN^- , N_3^- , or CN^- and, *in vivo*, it can be H_2O or OH^- . Anion-induced autoxidation with nucleophilic anion displacement of O_2 results in an intermediate ferrous heme/anion complex that acts as an electron donor to displace oxygen. Shikama [55,58] also demonstrated that, *in vacuo*, oxyheme is inherently stable and unlikely to dissociate $O_2^{\cdot-}$ spontaneously. Because O_2 is a poor one-electron acceptor, a considerable thermodynamic barrier exists for such an electron transfer. In aqueous media (*i.e.*, in contrast to *in vacuo*), oxyheme is subject to the nucleophilic attack of an entering water molecule (with or without proton catalysis) and to the attack of an entering hydroxide anion. These can cause irreversible oxidation of oxyheme to met-species with generation of $O_2^{\cdot-}$. Mb and Hb have therefore evolved with a globin moiety that can protect the $Fe(II)O_2$ center from the easy access of a water molecule (including its conjugate ions OH^- and H^+).

In an aqueous protein-free system, Kao and Wang [58] reported the oxidation of dipyrindine-ferrohemochrome by O_2 using a stopped-flow technique. The main pathway was interpreted to involve one O_2 molecule replacing one of the pyridine molecules in dipyrindine-ferrohemochrome to form an oxyheme and then undergoing decomposition of ferrohemochrome to ferrihemochrome and $O_2^{\cdot-}$. Unfortunately, the rate constant for this oxidation reaction could not be obtained because the concentration term of pyridine was always involved in its rate equation in a complicated manner. By numerical calculations, however, it follows that oxyheme autoxidation can proceed with a rate constant that is much higher than $1 s^{-1}$ in 0.1 M buffer, pH 8.5, at 25°C. If such an oxyheme is placed in a protein matrix, it would be protected against the nucleophilic attack of the solvent water molecule or hydroxyl ion so as to reduce its autoxidation by a factor of approximately 10^3 . This was the case in our study with denatured MbO_2 in 8 M urea (the details of which can be referred to in Sugawara et al. [59]). A globin moiety can act as a “breakwater” in aqueous media even in denatured conditions with 8 M urea. Furthermore, if an oxyheme is embedded in the native Mb architecture, MbO_2 acquires remarkable stability against oxyheme autoxidation by a factor of approximately 10^6 .

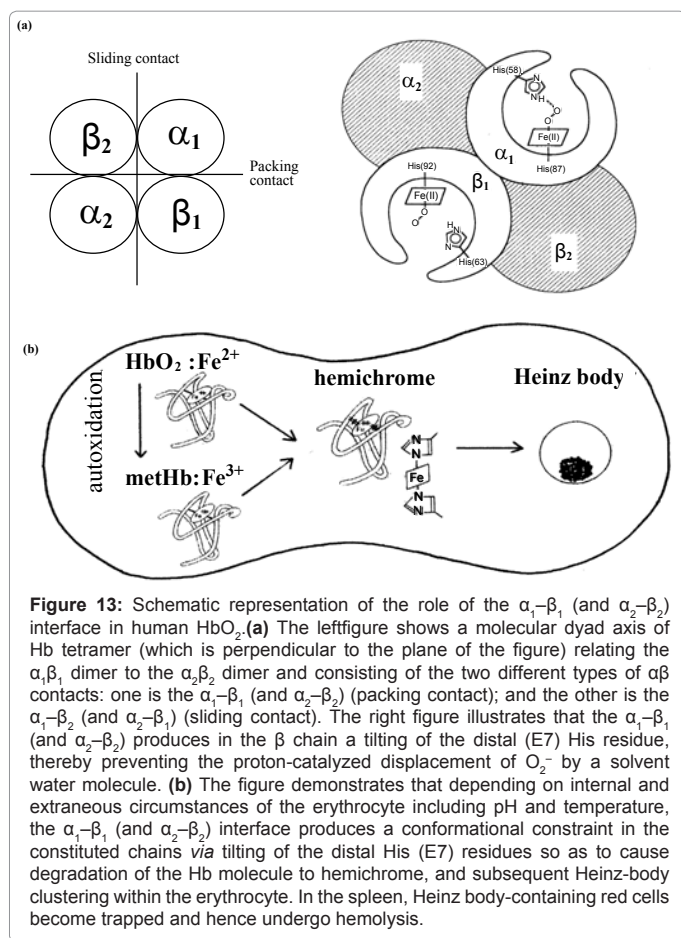
With regard to oxyheme stability in human HbO_2 , the half-life ($t_{1/2}$) was only 1.5 d in 0.1 M buffer and at physiological pH and temperature [34]. This is despite the fact that the content of metHb in normal red cells *in situ* [60,61] has been maintained to be less than or equal to 1% as a consequence of a NADH-dependent reducing system that can reduce the ferric-metHb resulting from autoxidation to deoxy-ferrous Hb [5-7]. However, as compared with the rates of monomeric mammalian Mbs, human HbO_2 seemed to be 2.2–3.6 times more stable against autoxidation (probably owing to its tetrameric architecture). Even though the autoxidation rate is a function of pH and temperature, the observed first-order rate constant was $0.0023 h^{-1}$ (12.6 d for $t_{1/2}$) for

human HbO_2 autoxidation under the conditions of 0.1 M buffer at pH 7.2 and 25°C in our study [35] because this value was calculated from the first rapid phase. Conversely, the relevant values of the monomeric mammalian Mbs were $0.0082 h^{-1}$ (3.5 d for $t_{1/2}$) for human MbO_2 , $0.0072 h^{-1}$ (4.0 d for $t_{1/2}$) for bovine MbO_2 , and $0.0050 h^{-1}$ (5.8 d for $t_{1/2}$) for sperm-whale MbO_2 under the same conditions used for human HbO_2 .

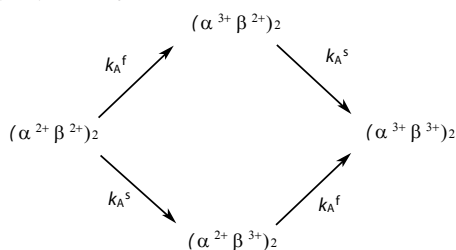
In our experiments, tetrameric human HbO_2 showed a biphasic autoxidation curve in acidic solutions in terms of the $-\ln([HbO_2]_t/[HbO_2]_0)$ versus time plot (Figure 4a); an initial rapid reaction (k_A^f) could be followed with a slower second phase (k_A^s). The difference in the rates between k_A^f and k_A^s decreased with increasing pH values of solutions, and finally disappeared (*i.e.*, k_A^f equal to k_A^s) if the pH of the solutions was more than 8 and became k_A^f equal to k_A^s . This finding leads to certain questions: how does the Hb molecule prompt the range of fast (k_A^f) and slow (k_A^s) components in acidic solutions? How does the molecule provoke k_A^f equal to k_A^s if the pH of solutions is more than 8? Does the biphasic autoxidation seen in acidic pH regions reflect a different rate owing to the individual Hb chains or the presence of valency hybrid intermediates such as $(\alpha^2\beta^3)_2$ and $(\alpha^3\beta^2)_2$?

A plot for the obtained values of k_A^f/k_A^s versus pH indicated that the reaction involves a single dissociation group of amino-acid residue with $pK_a=7.4$ (at 37°C) (Figure 4b), probably a His residue. In addition, study of rate measurement for the isolated α_{p-MB} and β_{p-MB} chains (and α_{SH} and β_{SH} chains) disclosed that once the constituted chains were isolated from the parent molecule, both separated chains could be oxidized much more rapidly to the ferric met-form over the measured pH range (5–10) when compared with the respective rates (k_A^f and k_A^s) of the parent molecules calculated from biphasic autoxidation curves as a reference (Figure 5). Also, there were no practical differences regarding the rate between the isolated individual chains (Figure 5). These findings may indicate that the individual chains have acquired considerable resistance to oxyheme autoxidation in their tetrameric protein architecture. It was also suggested that human HbO_2 seems to have acquired a “pH-sensitive molecular device” as a consequence of development of the tetrameric protein architecture. Hence, the molecule shows remarkable stability against oxyheme autoxidation more than in cases of isolated individual chains from the parent molecules and monomeric mammalian Mbs.

Moreover, our recent measurements (UV/VIS spectrophotometry, isoelectric-focusing electrophoresis, and polyacrylamide gel electrophoresis) for autoxidation of human HbO_2 [33] revealed that only two valency hybrids, *i.e.*, $(\alpha^3\beta^2)_2$ and $(\alpha^2\beta^3)_2$, emerged in the tetrameric HbO_2 autoxidation, even though, in theory, seven species of valency hybrids can be in existence during the reaction time course. These species are $(\alpha^2\alpha^2\beta^3\beta^2)$, $(\alpha^3\alpha^2\beta^2\beta^2)$, $(\alpha^2\beta^3)_2$, $(\alpha^3\beta^2)_2$, $(\alpha^2\alpha^3\beta^2\beta^3)$, $(\alpha^2\alpha^3\beta^3\beta^3)$ and $(\alpha^3\alpha^3\beta^3\beta^2)$. These had satisfactory-to-good consistency with those reported by Tomoda et al. [15,62-67]. Computer simulations on the basis of these measurements (UV/VIS spectrophotometry, isoelectric-focusing electrophoresis, and polyacrylamide gel electrophoresis) indicated that the relevant concentration progress curves derived from the subsequent tentative model could explain not only aspects of the spectrophotometric changes in terms of the $-\ln([HbO_2]_t/[HbO_2]_0)$ versus time plot, but also



aspects of the associated isoelectric-focusing electrophoretic profiles and polyacrylamide gel electrophoretic profiles, respectively, as shown below.



In an autoxidation reaction monitored in 0.05 M phosphate buffer (pH 5.0) at 37°C in the presence of 20% (v/v) glycerol, the following kinetic constants and molar fraction of the initial fast component (P) were established by least-squares fitting: $k_A^f = 0.148 \text{ h}^{-1}$ (4.7 h for $t_{1/2}$), $k_A^s = 0.0208 \text{ h}^{-1}$ (1.4 for $t_{1/2}$), and $P=0.51$. These findings led us to conclude that k_A^f represents intrinsic α -chain oxidation and k_A^s reflects intrinsic β -chain oxidation, and that the β chain manifests delayed autoxidation in human HbO_2 , which could be much more evident in acidic solutions.

Figure 13a shows our proposal with respect to this issue as reported in 1998 [30] and 2002 [31] in which we suggested a new function to the $\alpha_1\text{-}\beta_1$ (and $\alpha_2\text{-}\beta_2$) interface for stabilizing the HbO_2 tetramer against acidic autoxidation. That is, the $\alpha_1\text{-}\beta_1$ (and $\alpha_2\text{-}\beta_2$) interface produces a conformational constraint in the β chain whereby the distal (E7) His at position 63 is tilted slightly away from the bound O_2 so as to prevent

the proton-catalyzed displacement of O_2^- from the Fe(II)O_2 center by entrance of a water molecule. The β chain thus acquires a remarkably delayed oxidation rate in the HbO_2 tetramer. This is the origin of the chain heterogeneity seen in acidic solutions of HbO_2 autoxidation.

The most recent refinement of the crystallographic structure of human HbO_2 (where the O_2 molecule is clearly visible in the high-resolution electron density maps) demonstrated that the hydrogen bond made by His E7 β (*i.e.*, $\beta 63\text{His}$) is much weaker than that made by His E7 α (*i.e.*, $\alpha 58\text{His}$). However, it also substantiated that the geometry of the ligand and distal histidine is slightly different in the two subunits, with the O_2 atom lying $2.7 \pm 0.1 \text{ \AA}$ (10^{-1} nm) from the N^ϵ atom of the distal histidine in the α subunits, and $3.0\text{-}\text{\AA}$ away in the β subunits [68]. However, negligible changes were found for the $\alpha_1\text{-}\beta_1$ (and $\alpha_2\text{-}\beta_2$) interface with respect to examination of the crystal structure.

Similar phenomena suggesting participation of the $\alpha_1\text{-}\beta_1$ (and $\alpha_2\text{-}\beta_2$) interface (*i.e.*, participation of the inherent tilting capability of the distal (E7) His residues of the Hb molecule) garnered our interest. Our UV/VIS spectroscopic study suggested that human HbO_2 was highly susceptible to hemichrome formation even under physiological pH and temperature (Figure 1 and 2a) and, once isolated from the tetrameric parent molecule, the α ($\alpha_{\text{p-MB}}$) and β ($\beta_{\text{p-MB}}$) chains showed much higher susceptibilities to hemichrome when compared with the parent molecule (Figure 2b). In this regard, one must note that monomeric bovine heart Mb (MbO_2) did not show a propensity for hemichrome formation over a wide range of pH (4.5-10.5) and temperature from physiological to temperatures just before thermal unfolding (Figure 3).

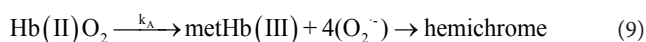
Heinz bodies are intra-erythrocytic inclusions of hemichrome formed as a result of Hb oxidation. They have been detected and characterized in drug-induced hemolytic anemia, defects in the intra-erythrocytic reducing system (*e.g.*, G-6-PD deficiency), and in unstable Hb disease [2,3]. Using unstable Hb disease as an example, several unstable Hbs have been reported. Regarding the molecular pathogenesis of unstable Hbs, it is known that the instability of labile Hb variants in patients can be attributed to amino-acid substitutions (or deletions). These disrupt and perturb the Hb structure via interference with α -helix formation, disruption of heme binding, or altered $\alpha_1\text{-}\beta_1$ (and $\alpha_2\text{-}\beta_2$) or $\alpha_1\text{-}\beta_2$ (and $\alpha_2\text{-}\beta_1$) contacts [2]. The consequent changes in circulating red cells in patients with unstable Hb disease include an inherent tendency towards irreversible denaturation of Hb or globin due to a defect in the amino-acid composition of labile Hb molecules, a continuous tendency toward hemichrome formation, precipitation or aggregation of Hb molecules resulting in buildup of the molecules to form Heinz bodies, and hemolysis.

Exposure of red cells to acetylphenylhydrazine and subsequent staining with crystal violet also revealed a greater abundance of Heinz bodies within G-6-PD-deficient cells compared with that in normal cells [69,70]. In addition, Sear et al. [71] and Campwala and Desforges [72] reported that Heinz bodies often appeared in normal-aging red cells, and that this age-related appearance of Heinz bodies was particularly pronounced in splenectomized individuals [73]. According to several authors [1,74,75], aged or damaged red cells affected by drugs may be "filtered off" by the spleen irrespective of whether or not they contain Heinz bodies in a similar manner to the filtering-off of red blood cells in patients with unstable Hb caused by unstable Hb hemolytic anemia.

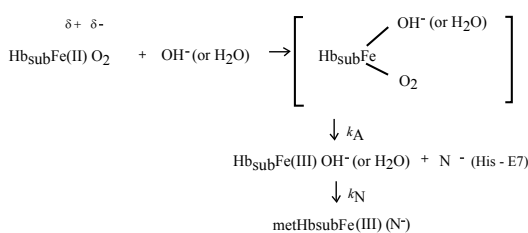
Using freshly drawn venous blood from healthy donors, we found that the number of Heinz bodies formed in red cells increased with increasing temperature when blood samples were subjected to mild heating at temperatures greater than 37°C for 30 min (Figures 6-9).

Under identical conditions of mild heating, we measured blood fluidity using a MC-FAN [32,33] because it involves a characteristic V-shaped groove array with micro flow paths (width, 7 μm; length, 30 μm; depth, 4.5 μm) engraved on a single-crystal silicon substrate in an integral circuit. When red cells passing through individual micro-channel arrays were monitored using an inverted metallographic microscope, images revealed good erythrocyte deformability when temperature-untreated samples were subjected to the MC-FAN (Figure 10a and 10b)). Conversely, a marked decline in erythrocyte deformability was observed in blood samples treated at temperatures more than 37°C for 30 min (Figure 10c). Temperature-treated samples also demonstrated an increased transit time for low transit sample volumes (Figure 11 and 12, Table 2). We therefore concluded that erythrocyte deformability decreased with increasing temperature of blood samples treated at temperatures above 37°C. The combination of our experimental findings and *in situ* observations suggests that instability leading to hemichrome formation is not only a peculiarity of labile Hb variants but is also an innate characteristic of physiologically normal Hb molecules.

In our experiments, the occurrence of hemichrome can be described as follows:

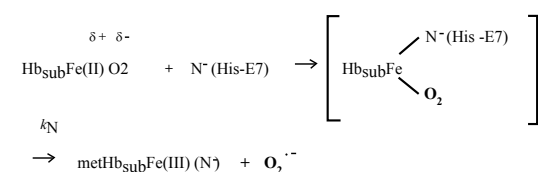


Taking into account the accepted framework of the S_N2 mechanism for autoxidation [54-58] and the accepted framework for hemichrome formation [13] in physiological conditions, hemichrome can form as follows:



In this scheme, Hb_{sub} represents each subunit of the Hb molecule. Nucleophilic displacement of O_2^- by entry of a water molecule or a hydroxyl ion should be the rate-limiting step. Also, the subsequent conversion of the met form into hemichrome by a heme ligand (N^-) endogenous to the protein must proceed very quickly with the kinetic relationship $k_N \gg k_A$. The most probable candidate for N^- in the HbA molecule is the N^ϵ -nitrogen of the distal His (E7) (i.e., the only amino-acid side chain in the ligand pocket) of each subunit because N^ϵ -nitrogen is located more than 4 Å (10^{-1} nm) from the iron in Hb, and is therefore not expected to coordinate in native Hb [13,76].

As described above, the content of metHb in normal erythrocytes [61,62] has been reported to be less than or equal to 1% by a NADH-dependent enzyme system [5-7]. This fact throws into question how erythrocytes can elicit the range of responses to hemichrome with such a small amount of metHb. We suggest that this can be achieved by intramolecular anion-induced nucleophilic displacement of molecular dioxygen *via* an intermediate ferrous heme/anion complex (a low-spin hemichrome) [17]. Such a reaction would follow the scheme:



In this reaction, nucleophilic displacement can be caused within the heme pocket by the N^ϵ -nitrogen of the distal His (E7) instead of nucleophilic incursion of the water molecule or the hydroxyl ion from outside the molecule. As indicated above, hemichrome formation occurs at every stage during the autoxidation of HbO_2 (i.e., initial, intermediate, and final) as a function of the pH and temperature of the solution. While the reaction proceeds along this scheme, hemichromes may be derived not only from HbO_2 species, but also from deoxyHb and metHb (Figure 13b). Vital hemichromes in erythrocytes *in situ* might arise from this intramolecular anion-induced nucleophilic displacement of O_2 via an intermediate ferrous heme/anion complex.

Our electron paramagnetic resonance (EPR) measurement study [30] showed a low-spin spectrum for the resulting oxidation products of isolated β chains with values of $g_1=2.77$, $g_2=2.27$, and $g_3=1.68$, in addition to the usual aquo-met species with g values of 5.86 and 1.99 under a magnetic field of 0–500 mT at 8.0 K in 10 mM maleate buffer (pH 6.2) and in the presence of 50% (*v/v*) glycerol. According to Rifkind et al. [13], such low-spin complexes characterized by the highest g values in the range 2.83–2.75 and the lowest g values in the range 1.69–1.63 have been designated as “complex B”, thereby indicating the crystal field parameters of the reversible hemichrome (i.e., a water-retained bis-histidine complex). The molar fraction of the hemichrome (complex B) in the oxidized β chains was estimated to be 85% at pH 6.2 because a low-spin species was in equilibrium with a high-spin species corresponding to the usual aquo-met species.

Interestingly, recent crystallographic and EPR spectroscopic studies concerning tetrameric Hbs isolated from the Antarctic fish species *Trematomus bernacchii*, *Trematomus newnesi*, and *Gymnodraco acuticeps* show that endogenous coordination at the sixth coordination site of the heme iron could be the bis-histidyl adducts in the ferric state in the solid and solution state [18,77-79]. In Antarctic fish, isolated Hbs are oxidized readily at room temperature to a partial hemichrome state in which only the iron of the β chain is bonded to the distal His. Such bis-histidyl coordination was also discovered in the crystals of horse metHb exposed to acidic pH (where the proximal His [His87(F8) α] and a water molecule are the axial heme ligands) to the hemichrome (bis-histidine) form (in which the proximal His and the distal His [His58(E7) α] are the axial heme ligands) [80]. In the case of horse metHb, the bis-histidyl coordination was seen in α chains but not in β chains. These crystal structures suggest a different binding state of α and β chains as well as a different pathway to hemichrome.

As described above, the α_1 - β_1 (and α_2 - β_2) interface seemed to have dual faces. One is for stabilizing the HbO_2 tetramer against the acidic autoxidation and the other is for controlling the fate (removal) of its own erythrocyte from the blood circulation. The α_1 - β_1 (and α_2 - β_2) interface produces a conformational constraint in the constructed chains of the Hb molecule *via* tilting of the distal (E7) His residues, i.e., $\alpha 58\text{His}$ (E7) in the α chain and $\beta 63\text{His}$ (E7) in the β chain. It was also shown that the α_1 - β_1 (and α_2 - β_2) interface appears to have a pH-sensor and a temperature-sensor. By virtue of these endowments, it seemed that Hb molecules can accomplish their roles not only as suitable O_2 carriers between the lungs and tissues but also as equipped “molecular sensors” within the erythrocyte to control the fate (removal) of their own erythrocytes from the blood circulation depending on internal and extraneous circumstances, including pH and temperature (Figure 13).

Regarding the latter issue, normal erythrocytes develop Heinz bodies late in their lifespan. A wide variety of biochemical changes have

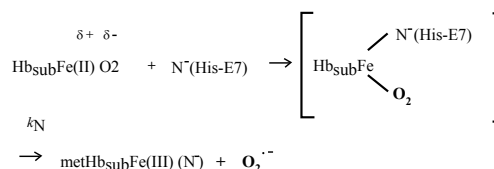
been reported to accompany the aging of red cells [81]. These include carboxymethylation of proteins, activation of proteases, glycosylation of proteins, loss of membrane area, decline in changes in the ratio of bands 4.1a to 4.1b, increases in oxidized lipids and proteins, changes in the rheology and fragility of cells, changes in the exposure of cell-surface sugars, and gradual accumulation of Ca^{2+} . Low [82] demonstrated that band-3 clustering might warrant closer scrutiny as a possible transducer of distress signals from the cytoplasm to the external surface of the cell because it can be caused by hemichrome binding, ATP depletion, malondialdehyde formation, Ca^{2+} accumulation, oxidative crosslinking, or weakening of the skeletal membrane. It is known that hemichromes formed within erythrocytes bind to the cytoplasmic portion of band 3 in the membrane. They then rapidly copolymerize with the soluble cytoplasmic domain of membrane band 3, forming an insoluble copolymer, followed by other changes involved in the pathogenesis of red-cell destruction [83-88]. The dominant role of band-3 clustering suggests that hemichrome formation-induced band-3 clustering could also provide a key to controlling the fate of senescent and damaged red cells in the blood circulation [84].

Discussion

Heinz bodies are intra-erythrocytic inclusions of hemichrome formed from oxidized or denatured Hb. They are commonly seen by phase contact microscopy as dark spots free in the cytoplasm or attached to the cytoplasmic surface of the erythrocyte membrane. Heinz bodies occur in red cells naturally under three distinct conditions. First, erythrocytes containing unstable Hbs, especially Hbs with mutations near the heme site in the β subunits, show elevated levels of Heinz bodies [2,3]. Second, Heinz bodies are seen in normal cells (containing normal Hb) under conditions of oxidant stress. The oxidant stress can arise either in cells suffering from a diminished capacity to maintain intracellular reducing power, e.g., in G-6-PD and glutathione peroxidase deficiency diseases [69,70]. Third, Heinz bodies often appear in normal cells as they age [71,72]. This age-related appearance of Heinz bodies is especially pronounced in splenoectomized individuals where a major organ of senescent cell removal has been excised [73]. Heinz body formation, however, whether natural or drug induced or oxidant stress promoted or unstable Hb disease produced, has considered to be occurred by a similar mechanism.

From this point of view, in this article, we made an attempt to propose a new mode of Heinz body formation mechanisms on the basis of our experimental accomplishments and the related current interpretations and arguments, wherein the inherent tilting capability of the distal (E7) His residues (*i.e.*, $\alpha 58\text{His}$ (E7) in the α chain and $\beta 63\text{His}$ (E7) in the β chain) of the Hb molecule plays a major role as well as involvement of the $\alpha_1-\beta_1$ (and $\alpha_2-\beta_2$) interface. As represented schematically in Figure 13, in this mechanisms, bis-histidylcoordination proficiency to the heme iron of the distal (E7) His residues can be prerequisite not only for an invocation to the end result of distal-side perturbations of the heme pocket against receipt for incoming stimuli around the molecule (*i.e.*, pH, temperature, oxidative stress), but also for the molecular biosensing mechanisms equipped in human erythrocytes for appreciation of cell aging and determination of their lifespan. Moreover this bis-histidyl coordination of the distal (E7) His residues to the heme iron can be manifested *via* collaboration of the $\alpha_1-\beta_1$ (and $\alpha_2-\beta_2$) interface of the Hb molecule. Practically, vital hemichromes in erythrocytes can be achieved by intramolecular anion-induced nucleophilic displacement of molecular dioxygen (O_2) via an intermediate ferrous heme/anion complex (a low-spin hemichrome)

by relying upon intrinsic tilting capability of the distal (E7) His residues (their bis-histidylcoordination proficiency to the heme iron):



In this reaction, nucleophilic displacement can be caused within the heme pocket by the N^{\ominus} -nitrogen of the distal His (E7) instead of nucleophilic incursion of the water molecule or the hydroxyl ion from outside the molecule. Hence, it was suggested that the sequential changes occurring within red corpuscles upon the removal of non-functional erythrocytes include: 1) receipt for internal and external stimuli (*i.e.*, pH, temperature, oxidative stress around the erythrocyte) via the $\alpha_1-\beta_1$ (and $\alpha_2-\beta_2$) interface of the molecule; 2) an invocation to distal-side perturbations of the heme pocket as the end result of the receipt of incoming stimuli; 3) temporal bis-histidyl coordination of the distal (E7) His residues to the heme iron that lead to hemichrome (degradation of the Hb molecule); 4) hemichrome emergence and subsequent hemichrome precipitation and aggregation of the Hb molecules that lead to formation of Heinz bodies within the erythrocyte; and 5) hemolysis of Heinz body-containing red cell in the spleen.

Therefore, in the following, in an attempt to clarify how our hypothesis can explain a diverse status of Heinz body formation within the erythrocytes, we assess these (either in natural or drug induced or oxidant stress promoted or unstable Hb disease produced) one by one in detail.

First of all, we take up unstable Hb disease, as over 90 different unstable Hbs have been reported so far [2,3]. In establishing a diagnosis of unstable Hb disease, the heat denaturation test is considered to be the single most important procedure, in which a fresh hemolysate is diluted into 50 volumes of buffer solution and heated at 60°C ; at intervals the precipitates are removed from samples by centrifugation, and the optical density of the supernatant is measured. The reason of such instability even on mild heating (*i.e.*, inclination toward accelerated degradation of Hb molecule to hemichrome resulting hemichrome precipitation and subsequent formation of Heinz bodies within the erythrocytes) is quite well understood at the molecular level, but there is still a lack of knowledge of the changes occurring during precipitation and ultimate cause of hemolysis.

Addition to this, the similarity to events observed in the oxidative hemolytic anemia suggests that the precipitation of unstable Hbs is accompanied by oxidative changes [2,3]. The oxidative hemolytic anemia arise either from formation of excess oxidizing products (as with acetylphenylhydrazine administration) or from breakdown of protective mechanisms against oxidants (as in G-6-PD deficiency). In either case, the end result is the same as with unstable Hbs; the precipitation of Hb, the formation of Heinz bodies, and hemolysis.

In our hypothesis, incoming stimuli of the erythrocyte (e.g., pH, temperature, oxidative stress), whether natural or drug induced or oxidant stress promoted or unstable Hb disease produced, can be transmitted ultimately to the distal-side perturbations of residues lining the distal side of the heme pocket *via* the $\alpha_1-\beta_1$ (and $\alpha_2-\beta_2$) interface, so that they let the distal (E7) His residues coordinate at the sixth coordination position of the heme iron to form a bis-histidyl complex.

This temporal bis-histidyl coordination by virtue of the inherent tilting capability of the distal (E7) His residues (*i.e.*, hemichrome emergence) in turn triggers a series of irreversible chemical reactions (including hemichrome formation-induced band-3 clustering and subsequent formation of Heinz bodies) that lead to the removal of non-functional erythrocytes from the blood circulation. Our hypothesis definitely demonstrates that there is positive correlation between the oxidative behavior of human Hb, its inseparably related instability (accelerated inclination toward degradation of Hb molecule to hemichrome), the subsequent formation of Heinz bodies within the erythrocyte and its ultimate fate (hemolysis) even on mild conditions at close-to-physiological temperatures and pH.

The defect in unstable Hbs involves important internal bonding amino acids, particularly those forming bonds with the heme group. Many of the mutants that occur at the α_1 - β_2 (and α_2 - β_1) interface have altered oxygen affinity, but the bulk of evidence suggests that the α_1 - β_1 (and α_2 - β_2) interface is much more important in maintaining the molecular stability of Hb than the α_1 - β_2 (and α_2 - β_1) interface. Hemolytic anemia results from substitutions affecting the α_1 - β_1 (and α_2 - β_2) interface or the heme pocket. If such mutations occur, the heme iron will be oxidized more readily, and a sequence of events leads to hemichrome formation and subsequent Heinz-body clustering in red cells that causes hemolytic anemia. Typical examples of such variants are summarized in Table 3. Surprisingly, almost all of these pathological mutations are found on the β chain, especially in the α_1 - β_1 (and α_2 - β_2) contact region: Tacoma [β 30(B12)Arg \rightarrow Ser], Abraham Lincoln [β 32(B14)Leu \rightarrow Pro], Castilla [β 32(B14)Leu \rightarrow Arg], Peterborough [β 111(G13)Val \rightarrow Phe], Madrid [β 115(G17)Ala \rightarrow Pro], Khartoum [β 124(H2)Pro \rightarrow Arg], J. Guantanamo [β 128(H6)Ala \rightarrow Asp] and Leslie [β 131(H9)Gln \rightarrow deleted]. In these Hbs, the α_1 - β_1 (and α_2 - β_2) interface would become loose or disruptive due to many different causes including: the insertion of proline (Abraham Lincoln, Madrid), the substitution with a too-small amino acid side chain (Tacoma) or a too-large side chain (Peterborough), the introduction of a charged or very polar group (Castilla, Khartoum, J. Guantanamo), and the deletion of amino acid residue (Leslie).

The situation in patients with G-6-PD deficiency [2,3] can serve as another example. Red cells are known to be vulnerable to injury by endogenous and exogenous oxidants. Oxidants can be inactivated by reduced glutathione in erythrocytes with normal G-6-PD activity because the pentose phosphate shunt supplies NADPH

(which is required for glutathione recycling). In G-6-PD-deficient erythrocytes, however, the reduced glutathione cannot be restored, and the cells sustain irreversible oxidative damage. However, G-6-PD deficiency produces symptoms only if the patient is exposed to an environmental factor that results in increased oxidative stress. Such stress includes antimalarials (e.g., primaquine, pamaquine, dapson), sulfonamides, nitrofurantoin and phenacetin. The resulting crisis can lead to hemolysis of up to 25–30% of red cells within hours. However, the crisis is self-limited, and only the older population of red cells is destroyed. The mechanisms responsible for such an acute hemolytic crisis in patients taking these drugs cannot be explained on the basis of conventional views. Figure 13 suggests that this crisis could be triggered by fluctuations in endogenous and exogenous oxidative stress under the fragile pentose phosphate shunt.

Malaria provides the other example. This is a protozoal disease transmitted by the bite of female *Anopheles* mosquitoes (*Plasmodium falciparum*, *P. malariae*, *P. vivax*, and *P. ovale*). Blackwater fever syndrome is caused by infection with *P. falciparum*, and is characterized by repeated bouts of chills and fevers, severe intravascular hemolysis and anemia, jaundice, hemoglobinuria (black urine) and splenic enlargement [89-91]. Patients often develop fevers above 40°C. A feature of this syndrome is that symptoms can be exacerbated in patients with G-6-PD deficiency as a result of taking quinine. In these patients, massive destruction of red cells infected by the parasite occurs, but similar numbers of normal erythrocytes are also ruptured, resulting in characteristic hemoglobinuria. The reason for the massive hemolysis of non-infected red cells is unclear. However, the possibility of a relationship between quinine ingestion and the associated massive hemolysis, as well as the relevance of G-6-PD deficiency, is addressed in Figure 13. Fevers above 40°C, endogenous G-6-PD deficiency, and exogenous quinine ingestion represent conditions that induce acute hemolysis, thereby leading to massive blood loss and hemoglobinuria.

Conclusions

Cellular life is reliant upon rapid and efficient responses to internal and external conditions whereby basic molecular events associated with these processes are the structural transitions of the proteins (structural protein allostery) involved. The human Hb molecule ($\alpha_2\beta_2$) holds a special position in these structural transitions. Hb has two types of α - β interface (*i.e.*, α_1 - β_1 [and α_2 - β_2] and α_1 - β_2 [and α_2 - β_1]). The latter α_1 - β_2 (and α_2 - β_1) interface is associated with cooperative O₂ binding, and exhibits principal roles if the molecule goes from its deoxygenated to oxygenated quaternary structure. However, the role of the former α_1 - β_1 (and α_2 - β_2) interface has been unclear for a long time.

In this regard, important and intriguing observations have been accumulating, so that a new gaze can be focused on the α_1 - β_1 (and α_2 - β_2) interface. In this article, on the basis of our experimental accomplishments and the related current interpretations and arguments, we first proposed a new mode of Heinz body formation mechanisms, wherein the inherent tilting capability of the distal (E7) His residues (*i.e.*, α 58His (E7) in the α chain and β 63His (E7) in the β chain) of the Hb molecule plays a major role as well as involvement of the α_1 - β_1 (and α_2 - β_2) interface. Specifically, the suggested sequential changes occurring within the erythrocyte upon the removal of non-functional erythrocytes, whether natural or drug induced or oxidant stress promoted or unstable Hb disease produced, include: 1) receipt for internal and external stimuli around the erythrocyte (e.g., pH, temperature, oxidative stress) via the α_1 - β_1 (and α_2 - β_2) interface of the molecule; 2) an invocation to distal-side perturbations of the heme

• E [β 26(B8)Glu \rightarrow Lys]	• Volga [β 27(B9)Ala \rightarrow Asp]
• Genova [β 28(B10)Leu \rightarrow Pro]	• St. Louis [β 28(B10)Leu \rightarrow Gln]
• Tacoma [β 30(B12)Arg \rightarrow Ser]	• Abraham Lincoln [β 32(B14)Leu \rightarrow Pro]
• Castilla [β 32(B14)Leu \rightarrow Arg]	• Philly [β 35(C1)Tyr \rightarrow Phe]
• Rush [β 101(G3)Glu \rightarrow Gln]	• Peterborough [β 111(G13)Val \rightarrow Phe]
• Madrid [β 115(G17)Ala \rightarrow Pro]	• Khartoum [β 124(H2)Pro \rightarrow Arg]
• J. Guantanamo [β 128(H6)Ala \rightarrow Asp]	• Wien [β 130(H8)Tyr \rightarrow Asp]
• Leslie [β 131(H9)Gln \rightarrow deleted]	• Torino [α 43(CD1)Phe \rightarrow Val]
• L. Ferrara [α 47(CD5)Asp \rightarrow Gly]	• Setif [α 94(G1)Asp \rightarrow Tyr]
• St. Lukes [α 95(G2)Pro \rightarrow Arg]	

Table 3: Unstable hemoglobin variants, showing sites of amino acid substitutions (or deletions), redrawn from Sugawara et al. [34]. Each individual row illustrates variant's name, the residue concerned (chain; number; position), and replacement (from \rightarrow to), respectively.

pocket as the end result of the receipt of incoming stimuli; 3) temporal bis-histidylcoordination of the distal (E7) His residue to the heme iron that lead to hemichrome (degradation of the Hb molecule); 4) hemichrome emergence and subsequent hemichrome precipitation and aggregation of the Hb molecules that lead to formation of Heinz bodies within the erythrocyte; and 5) hemolysis of Heinz body-containing red cell in the spleen.

Granting this new mode of Heinz body formation mechanisms to be basic premise, we then made an attempt to examine how this new mode of mechanisms can serve as a basis for deeper understanding of clinical aspects of drug-induced hemolytic anemia, defects in the intracellular reducing system and unstable Hb disease, in which the mechanisms for acute hemolytic crisis cannot be explained on the basis of conventional views. The followings were shown:

- (1) Almost all of pathological mutations of unstable Hbs are found on the β chain, especially in the α_1 - β_1 (and α_2 - β_2) contact region: Tacoma [$\beta 30$ (B12)Arg \rightarrow Ser], Abraham Lincoln [$\beta 32$ (B14)Leu \rightarrow Pro], Castilla [$\beta 32$ (B14)Leu \rightarrow Arg], Peterborough [$\beta 111$ (G13)Val \rightarrow Phe], Madrid [$\beta 115$ (G17)Ala \rightarrow Pro], Khartoum [$\beta 124$ (H2)Pro \rightarrow Arg], Guantanamo [$\beta 128$ (H6)Ala \rightarrow Asp] and Leslie [$\beta 131$ (H9)Gln \rightarrow deleted].
- (2) Acute hemolytic crisis observed in patients of G-6-PD deficiency while taking drugs such as antimalarials (e.g., primaquine, pamaquine, dapson), sulfonamides, nitrofurantoin and phenacetin can be explained by increased oxidative stress against inadequate reduced glutathione levels in erythrocytes of the patients.
- (3) Acute hemolytic crisis associated with black water fever syndrome of malarial patients caused by infection with *Plasmodium falciparum* can be also explained by fevers above 40°C, endogenous G-6-PD deficiency, and exogenous quinine ingestion.

References

1. WEISS L (1962) The structure of fine splenic arterial vessels in relation to hemoconcentration and red cell destruction. *Am J Anat* 111: 131-179.
2. Winslow RM, Anderson WF (1978) The Hemoglobinopathies. In *The Metabolic Basis of Inherited Disease*. Stanbury JB, Wyngaarden JB, Fredricks DS Eds.; McGraw-Hill Book Company: New York, NY, USA, 1465-1507.
3. Weatherall DJ, Clegg JB, Higgs DR, Wood WG (1995) The Hemoglobinopathies. In *The Metabolic and Molecular Basis of Inherited Disease*. Scriver CR, Beaudet AL, William SS, Valle D Eds.; McGraw-Hill Inc.: New York, NY, USA, Volume III, pp. 3413-3484.
4. Jacob HS (1970) Mechanisms of Heinz body formation and attachment to red cell membrane. *Semin Hematol* 7: 341-354.
5. Scott EM, Duncan IW, Ekstrand V (1965) The reduced pyridine nucleotide dehydrogenases of human erythrocytes. *J Biol Chem* 240: 481-485.
6. Hultquist DE, Passon PG (1971) Catalysis of methaemoglobin reduction by erythrocyte cytochrome B5 and cytochrome B5 reductase. *Nat New Biol* 229: 252-254.
7. Sugita Y, Nomura S, Yoneyama Y (1971) Purification of reduced pyridine nucleotide dehydrogenase from human erythrocytes and methemoglobin reduction by the enzyme. *J Biol Chem* 246: 6072-6078.
8. Rachmilewitz EA, Peisach J, Bradley TB, Blumberg WE (1969) Role of haemichromes in the formation of inclusion bodies in haemoglobin H disease. *Nature* 222: 248-250.
9. Rachmilewitz EA, Peisach J, Blumberg WE (1971) Studies on the stability of oxyhemoglobin A and its constituent chains and their derivatives. *J Biol Chem* 246: 3356-3366.
10. Rachmilewitz EA (1974) Denaturation of the normal and abnormal hemoglobin molecule. *Semin Hematol* 11: 441-462.
11. Winterbourn CC, Carrell RW (1974) Studies of hemoglobin denaturation and Heinz body formation in the unstable hemoglobins. *J Clin Invest* 54: 678-689.
12. Macdonald VW (1994) Measuring relative rates of hemoglobin oxidation and denaturation. *Methods Enzymol* 231: 480-490.
13. Rifkind JM, Abugo O, Levy A, Heim J (1994) Detection, formation, and relevance of hemichromes and hemochromes. *Methods Enzymol* 231: 449-480.
14. Brunori M, Falcioni G, Fioretti E, Giardina B, Rotilio G (1975) Formation of superoxide in the autoxidation of the isolated α and β chains of human hemoglobin and its involvement in hemichrome precipitation. *European Journal of Biochemistry* 53: 99-104.
15. Tomoda A, Sugimoto K, Suhara M, Takeshita M, Yoneyama Y (1978) Haemichrome formation from haemoglobin subunits by hydrogen peroxide. *Biochem J* 171: 329-335.
16. McDonald MJ, Turci SM, Mrabet NT, Himelstein BP, Bunn HF (1987) The kinetics of assembly of normal and variant human oxyhemoglobins. *J Biol Chem* 262: 5951-5956.
17. Sugawara Y, Kadono E, Suzuki A, Yukuta Y, Shibasaki Y, et al. (2003) Hemichrome formation observed in human haemoglobin A under various buffer conditions. *Acta Physiol Scand* 179: 49-59.
18. Vitagliano L, Vergara A, Bonomi G, Merlino A, Verde C, et al. (2008) Spectroscopic and crystallographic characterization of a tetrameric hemoglobin oxidation reveals structural features of the functional intermediate relaxed/tense state. *J Am Chem Soc* 130: 10527-10535.
19. Perutz MF (1970) Stereochemistry of cooperative effects in haemoglobin. *Nature* 228: 726-739.
20. Perutz MF (1972) Nature of haem-haem interaction. *Nature* 237: 495-499.
21. Perutz MF, Fermi G, Abraham DJ, Poyart C, Bursaux E (1986) Hemoglobin as a receptor of drugs and peptides: X-ray studies of the stereochemistry of binding. *J Am Chem Soc* 108: 1064-1078.
22. Imai K (1994) Adair fitting to oxygen equilibrium curves of hemoglobin. *Methods Enzymol* 232: 559-576.
23. Baldwin J, Chothia C (1979) Haemoglobin: the structural changes related to ligand binding and its allosteric mechanism. *J Mol Biol* 129: 175-220.
24. Fermi G, Perutz MF (1981) Haemoglobin and Myoglobin. Volume 2, Clarendon Press: Oxford, UK.
25. Dickerson RE, Geis I (1983) Hemoglobin: Structure, Function, Evolution and Pathology; The Benjamin/Cummings Publishing Co., Inc., Menlo Park, CA, USA, 176 pages.
26. Perutz MF (1990) Mechanisms of Cooperativity and Allosteric Regulation in Proteins; Cambridge University Press: Cambridge, UK.
27. Perutz MF, Wilkinson AJ, Paoli M, Dodson GG (1998) The stereochemical mechanism of the cooperative effects in hemoglobin revisited. *Annu Rev Biophys Biomol Struct* 27: 1-34.
28. Borgstahl GE, Rogers PH, Arnone A (1994) The 1.8 Å structure of carbonmonoxy-beta 4 hemoglobin. Analysis of a homotetramer with the R quaternary structure of liganded alpha 2 beta 2 hemoglobin. *J Mol Biol* 236: 817-830.
29. Levy A, Sharma VS, Zhang L, Rifkind JM (1992) A new mode for heme-heme interactions in hemoglobin associated with distal perturbations. *Biophys J* 61: 750-755.
30. Tsuruga M, Matsuoka A, Hachimori A, Sugawara Y, Shikama K (1998) The molecular mechanism of autoxidation for human oxyhemoglobin. Tilting of the distal histidine causes nonequivalent oxidation in the beta chain. *J Biol Chem* 273: 8607-8615.
31. Yasuda Jp, Ichikawa T, Tsuruga M, Matsuoka A, Sugawara Y, et al. (2002) The alpha 1 beta 1 contact of human hemoglobin plays a key role in stabilizing the bound dioxygen. *Eur J Biochem* 269: 202-211.
32. Sugawara Y, Hayashi Y, Shigemasa Y, Abe Y, Ohgushi I, et al. (2010) Molecular biosensing mechanisms in the spleen for the removal of aged and damaged red cells from the blood circulation. *Sensors (Basel)* 10: 7099-7121.

33. Sugawara Y, Yamada M, Ueno E, Okazaki M, Okamoto A, et al. (2011) New roles assigned to the α_1 - β_1 (and α_2 - β_2) interface of the human hemoglobin molecule from physiological to cellular. *Appl Sci* 1: 13-55.
34. Sugawara Y, Sakoda M, Shibata N, Sakamoto H (1993) Autoxidation of human hemoglobin: kinetic analysis of the pH-profile. *Jpn J Physiol* 43: 21-34.
35. Goto T, Shikama K (1974) Autoxidation of native oxymyoglobin from bovine heart muscle. *Arch Biochem Biophys* 163: 476-481.
36. Brooks J (1948) The oxidation of haemoglobin to methaemoglobin by oxygen. *J Physiol* 107: 332-335.
37. Brooks J (1935) The oxidation of haemoglobin to methaemoglobin by oxygen II—The relation between the rate of oxidation and the partial pressure of oxygen. *Proceedings of the Royal Society of London Series B, Biological Sciences* 118: 560-570.
38. Mansouri A, Winterhalter KH (1973) Nonequivalence of chains in hemoglobin oxidation. *Biochemistry* 12: 4946-4949.
39. Tomoda A, Yoneyama Y, Tsuji A (1981) Changes in intermediate haemoglobins during autoxidation of haemoglobin. *Biochem J* 195: 485-492.
40. Hermans J Jr, Rialdi G (1965) Heat of ionization and denaturation of sperm-whale myoglobin determined with a microcalorimeter. *Biochemistry* 4: 1277-1281.
41. Fasman GD (1976) Physical and chemical data. In *Handbook of Biochemistry and Molecular Biology*, 3rd edition, CRC Press: Cleveland, OH, USA, p. 220.
42. Demetriou JA, Drewes, PA, Gin JB (1974) Enzymes. In *Clinical Chemistry*, 2nd ed.; Henry, R.J., Cannon, D.C., Winkelman, J.W., Eds.; Harper & Row Publishers: New York, NY, USA 815-1001.
43. Bauer JD (1980) Laboratory investigation of hemoglobin. In *Gradwohl's Clinical Laboratory Methods and Diagnosis*. Sonnenwirth, AC Jarett, L., Eds 809-901.
44. Kikuchi Y, Sato K, Ohki H, Kaneko T (1992) Optically accessible microchannels formed in a single-crystal silicon substrate for studies of blood rheology. *Microvasc Res* 44: 226-240.
45. Suganuma H, Inakuma T, Kikuchi Y (2002) Amelioratory effect of barley tea drinking on blood fluidity. *J NutrSciVitaminol (Tokyo)* 48: 165-168.
46. Begum AN, Terao J (2002) Protective effect of quercetin against cigarette tar extract-induced impairment of erythrocyte deformability. *J Nutr Biochem* 13: 265-272.
47. Kamada H, Hattori K, Hayashi T, Suzuki K (2004) In vitro evaluation of blood coagulation activation and microthrombus formation by a microchannel array flow analyzer. *Thromb Res* 114: 195-203.
48. Sumino H, Nara M, Seki K, Takahashi T, Kanda T, et al. (2005) Effect of antihypertensive therapy on blood rheology in patients with essential hypertension. *J Int Med Res* 33: 170-177.
49. Watanabe N, Kimura F, Kojima F, Endo, Y, Fujimoto, K et al. (2005) Effect of sterols in dietary fats on whole blood viscosity of stroke-prone spontaneously hypertensive rats (SHRSP) *J Oleo Sci* 54: 1-6.
50. Muranaka Y, Kunimoto F, Takita J, Sumino H, Nara M, et al. (2006) Impaired blood rheology in critically ill patients in an intensive care unit. *J Int Med Res* 34: 419-427.
51. Seki K, Sumino H, Nara M, Ishiyama N, Nishino M, et al. (2006) Relationships between blood rheology and age, body mass index, blood cell count, fibrinogen, and lipids in healthy subjects. *Clin HemorheolMicrocirc* 34: 401-410.
52. Watanabe N, Watanabe Y, Kumagai M, Fujimoto K (2009) Administration of dietary fish oil capsules in healthy middle-aged Japanese men with a high level of fish consumption. *Int J Food SciNutr* 60 Suppl 5: 136-142.
53. Shikama K (1985) Nature of the FeO₂ bonding in myoglobin: an overview from physical to clinical biochemistry. *Experientia* 41: 701-706.
54. Shikama K (1988) Stability properties of dioxygen-iron (II) porphyrins: An overview from simple complexes to myoglobin. *Coord Chem Rev* 83: 73-91.
55. Shikama K (1990) Autoxidation of oxymyoglobin: a meeting point of the stabilization and the activation of molecular oxygen. *Biol Rev Camb Philos Soc* 65: 517-527.
56. Shikama K (1998) The Molecular Mechanism of Autoxidation for Myoglobin and Hemoglobin: A Venerable Puzzle. *Chem Rev* 98: 1357-1374.
57. Shikama K (2006) Nature of the FeO₂ bonding in myoglobin and hemoglobin: A new molecular paradigm. *Prog Biophys Mol Biol* 91: 83-162.
58. Kao OHW, Wang JH (1965) Kinetic study of the oxidation of ferrohemeochrome by molecular oxygen. *Biochemistry* 4: 342-347.
59. Sugawara Y, Matsuoka A, Kaino A, Shikama K (1995) Role of globin moiety in the autoxidation reaction of oxymyoglobin: effect of 8 M urea. *Biophys J* 69: 583-592.
60. Paul WD, Kemp CR (1944) Methemoglobin: A normal constituent of blood. *Proc Soc Exp Biol Med* 56: 55-56.
61. BODANSKY O (1951) Methemoglobinemia and methemoglobin-producing compounds. *Pharmacol Rev* 3: 144-196.
62. Tomoda A, Takeshita M, Yoneyama Y (1978) Characterization of intermediate hemoglobin produced during methemoglobin reduction by ascorbic acid. *J Biol Chem* 253: 7415-7419.
63. Tomoda A, Tsuji A, Matsukawa S, Takeshita M, Yoneyama Y (1978) Mechanism of methemoglobin reduction by ascorbic acid under anaerobic conditions. *J Biol Chem* 253: 7240-7243.
64. Tomoda A, Yubisui T, Tsuji A, Yoneyama Y (1979) Kinetic studies on methemoglobin reduction by human red cell NADH cytochrome b5 reductase. *J Biol Chem* 254: 3119-3123.
65. Tomoda A, Imoto M, Hirano M, Yoneyama Y (1979) Analysis of met-form haemoglobins in human erythrocytes of normal adults and of a patient with hereditary methaemoglobinaemia due to deficiency of NADH-cytochrome b5 reductase. *Biochem J* 181: 505-507.
66. Tomoda A, Tsuji A, Yoneyama Y (1980) Mechanism of hemoglobin oxidation by ferricytochrome c under aerobic and anaerobic conditions. *J Biol Chem* 255: 7978-7983.
67. Tomoda A, Ida M, Tsuji A, Yoneyama Y (1980) Mechanism of methaemoglobin reduction by human erythrocytes. *Biochem J* 188: 535-540.
68. Park SY, Yokoyama T, Shibayama N, Shiro Y, Tame JR (2006) 1.25 Å resolution crystal structures of human haemoglobin in the oxy, deoxy and carbonmonoxy forms. *J Mol Biol* 360: 690-701.
69. JANDL JH, ENGLE LK, ALLEN DW (1960) Oxidative hemolysis and precipitation of hemoglobin. I. Heinz body anemias as an acceleration of red cell aging. *J Clin Invest* 39: 1818-1836.
70. Peisach J, Blumberg WE, Rachmilewitz EA (1975) Detection of formation, and relevance of hemichromes and hemochromes. *Biochim Biophys Acta* 393: 404-418.
71. Sears DA, Friedman JM, White DR (1975) Binding of intracellular protein to the erythrocyte membrane during incubation: the production of Heinz bodies. *J Lab Clin Med* 86: 722-732.
72. Campwala HQ, Desforges JF (1982) Membrane-bound hemichrome in density-separated cohorts of normal (AA) and sickled (SS) cells. *J Lab Clin Med* 99: 25-28.
73. Selwyn JG (1955) Heinz bodies in red cells after splenectomy and after phenacetin administration. *Br J Haematol* 1: 173-183.
74. Weiss L (1963) The Structure of Intermediate Vascular Pathways in the Spleen of Rabbits. *Am J Anat* 113: 51-91.
75. Wennberg E, Weiss L (1968) Splenic erythroclasia: an electron microscopic study of hemoglobin H disease. *Blood* 31: 778-790.
76. Phillips SE (1978) Structure of oxymyoglobin. *Nature* 273: 247-248.
77. Vitagliano L, Bonomi G, Riccio A, di Prisco G, Smulevich G, et al. (2004) The oxidation process of Antarctic fish hemoglobins. *Eur J Biochem* 271: 1651-1659.
78. Vergara A, Franzese M, Merlino A, Vitagliano L, Verde C, et al. (2007) Structural characterization of ferric hemoglobins from three antarctic fish species of the suborder notothenioidae. *Biophys J* 93: 2822-2829.
79. Vergara A, Franzese M, Merlino A, Bonomi G, Verde C, et al. (2009) Correlation between hemichrome stability and the root effect in tetrameric hemoglobins. *Biophys J* 97: 866-874.

80. Robinson VL, Smith BB, Arnone A (2003) A pH-dependent aquomet-to-hemichrome transition in crystalline horse methemoglobin. *Biochemistry* 42: 10113-10125.
81. Clark MR (1988) Senescence of red blood cells: progress and problems. *Physiol Rev* 68: 503-554.
82. Low PS (1991) Role of Hemoglobin Denaturation and Band 3 Clustering in Initiating Red Cell Removal. In *Red Blood Cell Aging*; Magnani 173-183.
83. Walder JA, Chatterjee R, Steck TL, Low PS, Musso GF, et al. (1984) The interaction of hemoglobin with the cytoplasmic domain of band 3 of the human erythrocyte membrane. *J Biol Chem* 259: 10238-10246.
84. Waugh SM, Low PS (1985) Hemichrome binding to band 3: nucleation of Heinz bodies on the erythrocyte membrane. *Biochemistry* 24: 34-39.
85. Low PS, Waugh SM, Zinke K, Drenckhahn D (1985) The role of hemoglobin denaturation and band 3 clustering in red blood cell aging. *Science* 227: 531-533.
86. Schlüter K, Drenckhahn D (1986) Co-clustering of denatured hemoglobin with band 3: its role in binding of autoantibodies against band 3 to abnormal and aged erythrocytes. *Proc Natl Acad Sci U S A* 83: 6137-6141.
87. Waugh SM, Walder JA, Low PS (1987) Partial characterization of the copolymerization reaction of erythrocyte membrane band 3 with hemichromes. *Biochemistry* 26: 1777-1783.
88. Zhang D, Kiyatkin A, Bolin JT, Low PS (2000) Crystallographic structure and functional interpretation of the cytoplasmic domain of erythrocyte membrane band 3. *Blood* 96: 2925-2933.
89. Van den Ende J, Coppens G, Verstraeten T, Van Haegenborgh T, Depaetere K, et al. (1998) Recurrence of blackwater fever: triggering of relapses by different antimalarials. *Trop Med Int Health* 3: 632-639.
90. Mararia WJM (2003) In *Manson's Tropical Diseases*. Cook GC, Zumura AI., Eds. W.B. Saunders: Philadelphia, USA 1205-1295.
91. Hue NT, Charlieu JP, Chau TT, Day N, Farrar JJ, et al. (2009) Glucose-6-phosphate dehydrogenase (G6PD) mutations and haemoglobinuria syndrome in the Vietnamese population. *Malar J* 8: 152.